

RESEARCH TECHNIQUES in NONDESTRUCTIVE TESTING

Volume VIII

p. 333 contains
a reference to
Grindo - Sodic

Edited by

R. S. SHARPE

Nondestructive Testing Centre

Atomic Energy Research Establishment

Harwell, Oxfordshire



1985

ACADEMIC PRESS

(Harcourt Brace Jovanovich, Publishers)

London Orlando San Diego New York

Toronto Montreal Sydney Tokyo

CHAPTER 7

Vibration Techniques in Nondestructive Testing

R. D. ADAMS

Department of Mechanical Engineering, University of Bristol, Bristol, UK

and

P. CAWLEY

Department of Mechanical Engineering, Imperial College, London, UK

I. Introduction	304
II. Vibration properties of materials	305
A. Metals	305
B. Composites	312
C. Effect of cracks and other damage on the damping and modulus	315
III. Vibration characteristics of structures	318
A. Single degree of freedom system	318
B. Continuous structures	322
C. Effect of defects	327
IV. Methods of measuring the natural frequencies and damping characteristics of specimens and structures	327
A. Steady-state methods	328
B. Transient methods	329
V. Global methods.	332
A. Natural frequency measurements	332
B. Damping measurements	339
C. Use of combined natural frequency and damping measurements	342
D. Discussion of global methods	342
VI. Local measurements	343
A. Excitation at a single point	343
B. Excitation at each test point	347
C. General assessment of local measurement techniques	355
VII. Conclusions	356
References	357

could this

I. INTRODUCTION

Vibration techniques for nondestructive testing have been used for hundreds, probably thousands, of years; yet the subject is still in its infancy. A standard technique for testing earthenware cooking pots has always been to tap them and listen to the ring. A good pot will produce a sustained, clear note while a cracked pot will sound "dead". The same technique is used in the crystal glass industry. The railway wheel tapper used to walk along the train tapping each wheel in turn. Again, cracked wheels did not ring as long as good ones. The test, which in this paper is termed the "wheel-tap" test is "global" since the whole component is tested by a tap at a single point. It is therefore a very rapid inspection method.

A superficially very similar technique is regularly used for testing laminated structures such as bonded panels. This is the "coin-tap" test which involves tapping each part of the panel with a coin. Again, a defective area sounds "dead". Defects such as adhesive disbonds, delaminations in composite materials and defective honeycomb construction can be detected by a skilled operator. The method is not suitable for the detection of transverse cracks (i.e., cracks running normal to the surface which is tapped). The coin-tap test is frequently confused with the wheel-tap technique but operates on a quite different principle. The coin-tap test is a local test which will only detect defects at the location of the tap. Therefore if the whole structure is to be tested, each part of it must be tapped and the test is much more time consuming than the wheel-tap method. However, the local test is more sensitive to certain types of defect and the two tests have quite different areas of application.

In the wheel-tap test, the operator detects differences in the pitch (frequency) and decay rate (damping) of the sound produced when good and defective wheels are struck. The test therefore depends on changes in the natural (resonant) frequencies and damping of the wheel with damage. These are properties of the whole wheel and do not depend on the position of excitation. Analysis of the vibration or sound waveform produced by a tap is a very attractive means of obtaining these properties, but, unfortunately, the human ear cannot achieve great accuracy or reliability. Until recently, the electronic equipment required to carry out the test was prohibitively expensive and bulky. Apart from a few specialist cases, the test has therefore remained subjective which has severely limited its application.

There are many other methods for measuring natural frequencies and damping, some of which have been applied to nondestructive testing. [See, for example, Uygur (1980).] However, in most cases, they are not as quick and convenient as the tap test and they have not found widespread

use. With the advent of microelectronics, the cost and size of the equipment required to extract the natural frequencies and damping from the sound produced by a tap has been greatly reduced so it is anticipated that there will be an upsurge of interest in the technique. The previous results are still relevant, however, since the reported natural frequency and damping changes are independent of the method of measurement. Valuable information regarding the sensitivity of the technique and likely application areas can therefore be obtained.

After reviewing the vibration properties of materials and structures, this chapter discusses different methods for measuring vibration properties. Reports of "global" tests based on natural frequency and damping measurements are discussed in section V. These are not classified according to the particular method used for measuring the properties.

The advent of microelectronics has also produced new opportunities in the field of local measurements, which are discussed in section VI. For example, an automated version of the coin-tap test has been developed. A variety of local properties may be measured, some of which require excitation at a single point of the structure, measurements being taken at each point of interest, and others which require both excitation and measurement at each test point. Section VI is divided into these categories.

The tests described here use frequencies of vibration which are mainly in the sonic range which extends up to 20 kHz. This chapter covers nondestructive inspection techniques in which vibration excitation is deliberately applied to the test structure. Many techniques for the condition monitoring of running machinery use measurements of the vibration levels on the machine during operation. These methods fall outside the scope of this chapter.

II. VIBRATION PROPERTIES OF MATERIALS

A. Metals

To cover the dynamic properties of all materials is beyond the limited scope of this chapter. We will therefore restrict the treatment to those materials which are to be found in stress-bearing situations in modern engineering. Metals and their alloys (referred to simply as metals from now on) provide the largest group of materials, but polymers, and particularly fibre reinforced composites, are becoming increasingly used in high-performance engineering. We will therefore treat metals and composites as two separate groups. Unreinforced polymers will not be covered here.

The vibration properties which concern us are the damping and the dynamic modulus. These are defined in Fig. 1. When taken round a stress cycle, all materials show a nonsingular relationship between stress and

could this

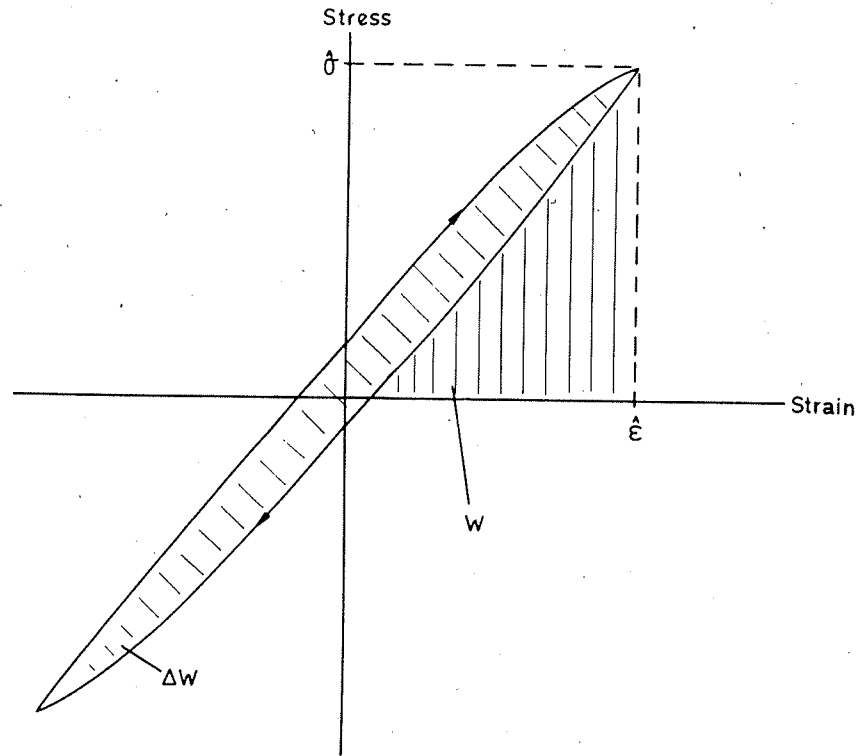


FIG. 1. Definition of specific damping capacity $\psi = \Delta W/W$, where $W = \sigma^2/2E = E\epsilon^2/2$.

strain. The modulus is given by the mean slope of the stress-strain loop. For most materials, there is little ambiguity in this definition, since the loop is almost indistinguishable from a straight line. The area ΔW of the loop represents the work done against internal friction and is the amount of energy dissipated during the cycle. There are many mechanisms which account for this energy loss (Birchon, 1964) although the main ones in metals are magnetomechanical interactions and microplastic straining. Referring to Fig. 1, it can be seen that the maximum strain energy stored per unit volume in the cycle is $W = \sigma^2/2E = E\epsilon^2/2$, where E is Young's modulus. We now define the specific damping capacity ψ of the material as $\psi = \Delta W/W$. This quantity is usually expressed as a percentage.

The damping capacity ψ is related to other commonly used damping parameters by the relationships

$$\psi = 2\pi/Q = 2\delta = 2\pi\eta = 4\pi c = 2\pi[(\omega_2 - \omega_1)/\omega_n],$$

where Q is the quality (amplification) factor, δ the logarithmic decrement, η the loss factor, c the proportion of critical damping, ω_n the natural frequency and ω_1 and ω_2 the half-power points (see section IV).

There is a wide range of damping values to be found in engineering materials, although usually the amount of damping available is small. There are some important exceptions, notably the cast irons, manganese-copper alloys, and some nickel-based alloys (Adams, 1972a; Adams and Fox, 1973; Cocharadt, 1953; Goodwin, 1968). Also, the damping is usually stress-dependent, as is shown for a range of materials in Fig. 2.

In steels, for instance, the damping is essentially due to magnetoelastic effects and is very dependent on the heat treatment as well as the cyclic stress level (Adams, 1972b). Characteristically, the damping increases from low stresses, reaches a peak and then decreases before microplastic straining at the onset of fatigue leads to a rapid increase of damping. This behaviour is shown in Fig. 3 for a 0.23% plain carbon steel in various states of heat treatment. Thus, we have already a possible means of nondestructively evaluating the condition of a steel specimen providing accurate damping measurements can be made on it. However, the elastic moduli of steel (Young's or shear) change but little with heat treatment or carbon content, and even less with cyclic stress. Adams (1972b) quotes a range of E values from 211 GPa to 209 GPa for carbon contents ranging from 0.12 to 0.985% and a wide range of heat treatments. An unpublished result by the same author gave an E value as low as 203 GPa for an extremely hard condition (diamond pyramid hardness number of 760). However, the variation in modulus is still small compared with that of the damping making the latter a much more sensitive indicator of material condition.

In steels, magnetic and mechanical hardness are related via the internal stresses of the material. One manifestation of this is the possibility of relating the height of the damping peaks ψ_p (such as those shown in Fig. 3), with the carbon content (Fig. 4); this diagram also shows the correlation with carbon content of the stress σ_p at which the damping peak occurs for annealed plain carbon steels.

Similar correlations of damping with metallurgical condition occur with other metals, but these are not widely documented and again there is little change in modulus. The main exception to this is cast iron, the dynamic properties of which have been given by Adams and Fox in several publications (Fox and Adams, 1972, 1973; Adams and Fox, 1973). Unlike most metals, cast iron may be regarded as a composite rather than an alloy, and has a range of Young's and shear moduli far in excess of other groups (e.g., steels, brasses, etc.). For the low-strength, coarse-flake graphite irons, an E value of 86 GPa was given by Fox and Adams (1973) while, for the high-strength nodular (spheroidal graphite) irons, an E value of

could this

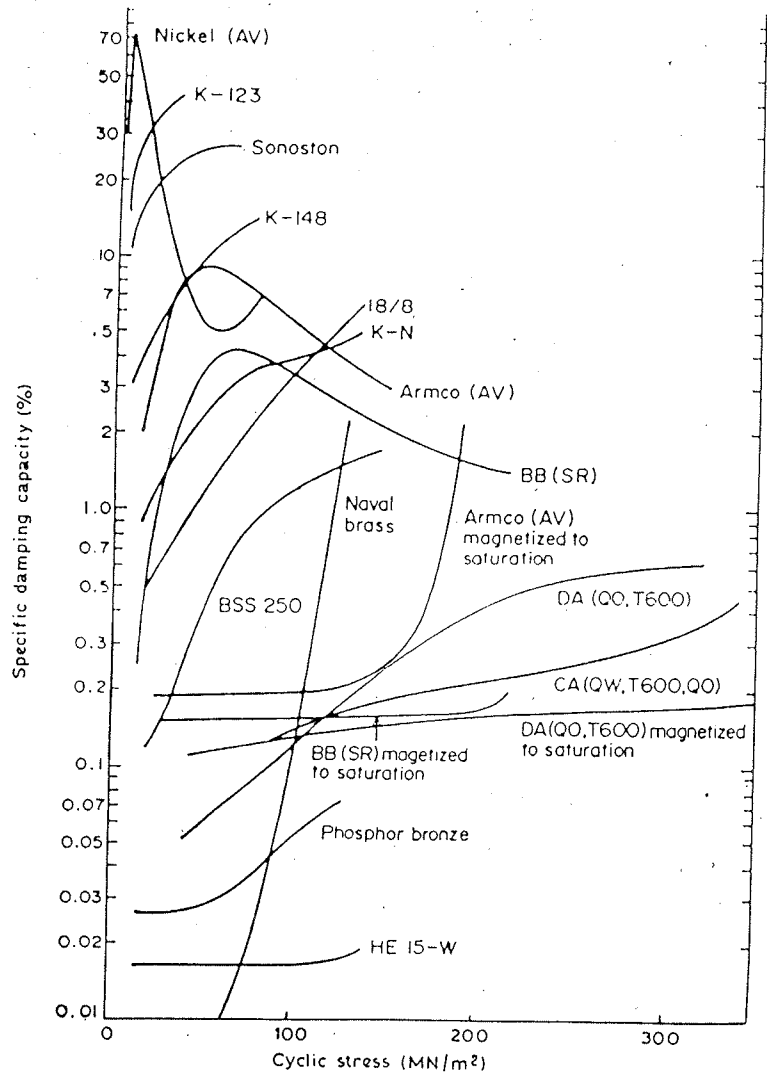


FIG. 2. Damping versus stress for a range of ferrous and nonferrous metals. Nickel (AV): annealed in vacuum; K-123, K-148, K-N: grades of cast iron; 18/8: stainless steel; Armco (AV): low carbon iron, annealed in vacuum; BB(SR): 0.12% carbon steel, stress relieved; BSS 250, Naval brass, phosphor bronze: copper-based alloys; CA, DA: high-carbon steels; HE 15-W: Duralumin aluminium alloy. [From Adams (1972a). With permission from *J. Sound Vibration* 23(2), 199-216. Copyright 1972 by Academic Press Inc. (London) Ltd.]

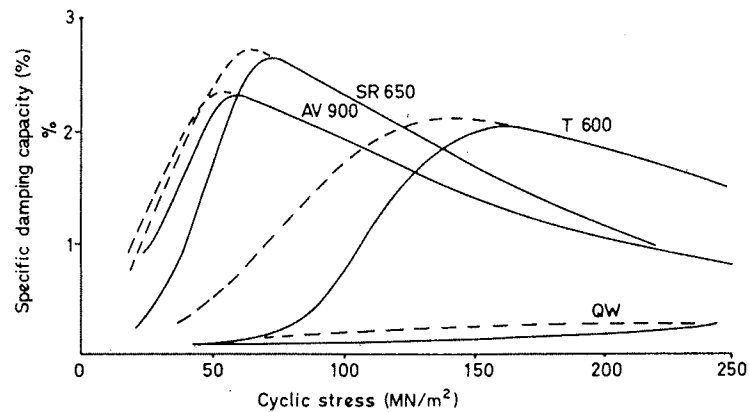


FIG. 3. Effect of heat treatment on the damping-stress relationship for 0.23% C steel. Full curves for increasing stress, broken curves for decreasing stress. AV 900, annealed in vacuum at 900°C; SR 650, stress relieved at 650°C; QW, quenched in water; T 600, tempered at 600°C. [From Adams (1972b).]

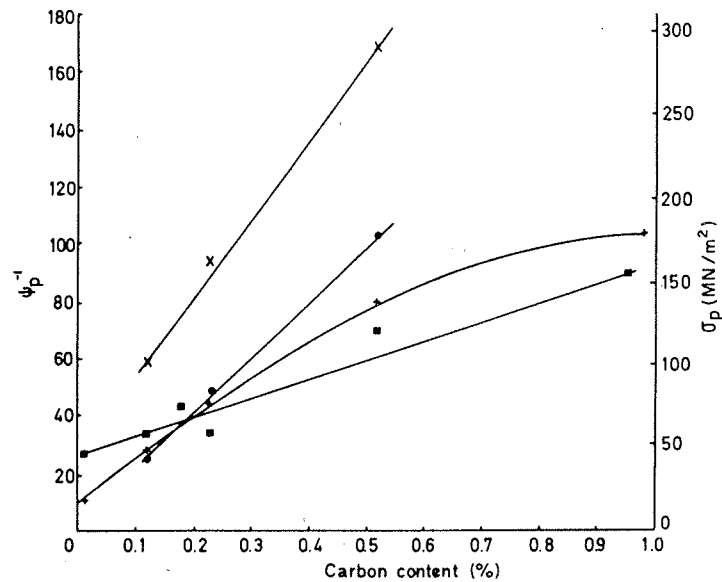


FIG. 4. Reciprocal of damping peak ψ_p^{-1} and stress at damping peak σ_p against carbon content. +: ψ_p^{-1} , annealed in vacuum; ●: ψ_p^{-1} , quenched in water, tempered at 600°C; ■: σ_p , annealed in vacuum; ×: σ_p , quenched in water, tempered at 600°C. [From Adams (1972b).]

could this

169 GPa, not much less than that of steel, was measured. This range of almost 2:1 in moduli is exceptional and is due to the change in shape of the graphite inclusions from the coarse-flake, through the fine-flake to the spherical form. Similarly, there is a wide range of damping values available, the coarse-flake graphite irons having the highest damping and the nodular irons the lowest. There is also a change in the dominant damping mechanism from micro-slipping within the graphite flakes towards magneto-mechanical effects in the nodular irons, although both mechanisms exist

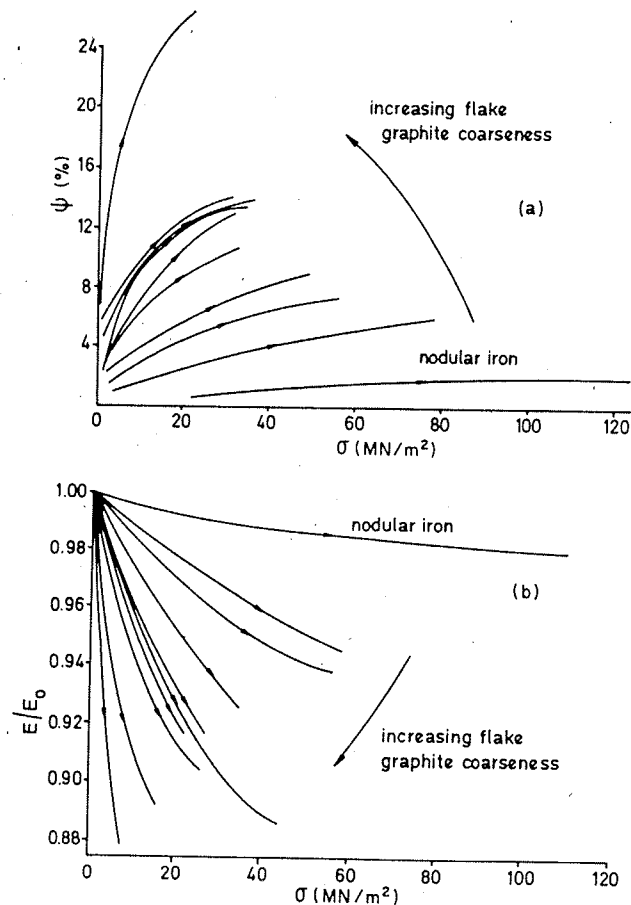


FIG. 5. Nonlinear dynamic behaviour of cast iron: (a) specific damping capacity ψ versus cyclic stress; (b) modulus ratio E/E_0 versus cyclic stress. [From Adams and Fox (1973).]

for all irons (Adams and Fox, 1973). Cast irons with an austenitic matrix (containing 20–40% nickel and up to 3% chrome) do not exhibit magneto-mechanical damping.

There are several additional points to be noted in connection with cast irons. For instance, the matrix may be ferritic, pearlitic, or some combination of the two, and both the damping and the modulus are markedly stress dependent. This stress dependence decreases as the graphite shape changes from coarse to fine flake, and then to the spheroidal form (Fig. 5). Also, when defining the modulus, it is necessary to identify the cyclic stress at which it is measured (effectively a secant modulus). This has given rise to the definition of E_0 , the modulus at very low cyclic stresses. It is best to measure E_0 ultrasonically or by very low-amplitude resonant vibration. Since E_0 varies with metallurgical condition, it provides a readily measured parameter.

Fox and Adams (1973) related damping and modulus to various strength parameters for cast irons and so extended the range of possibilities for nondestructive testing over the simple and often-used E_0 -strength correlation (see, for example, Fig. 6).

Damping measurements are of less application to high-strength (e.g., spheroidal graphite) cast irons because the damping is quite small and magneto-mechanical effects contribute a large proportion of the energy dissipation (Adams and Fox, 1973). Thus, the effectiveness of damping

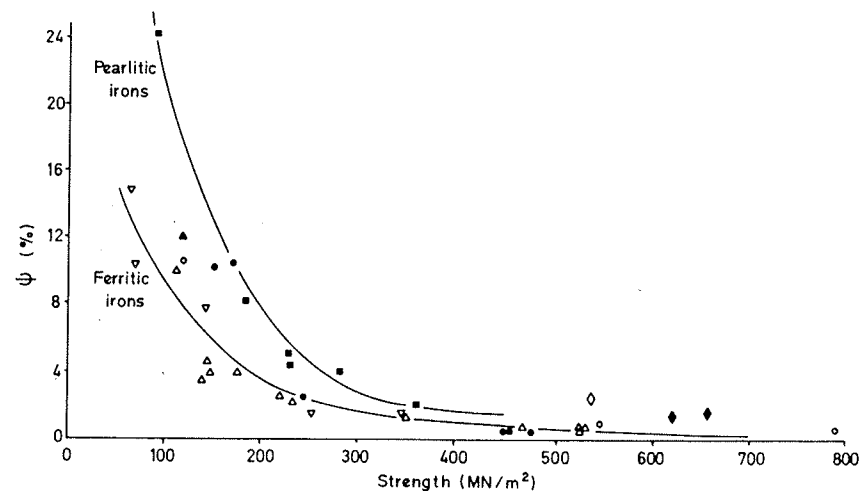


FIG. 6. Damping at 10% tensile strength versus tensile strength for a range of cast irons. [From Fox and Adams (1973).]

could this

tests in discriminating small changes in condition becomes much less marked for these fibres, the same is also true for the sonic modulus test.

B. Composites

High-performance composite materials consisting of high-strength reinforcing fibres embedded in a matrix which is usually resin based are finding increasing application in critical load bearing areas where NDT is essential.

The dynamic modulus of the material is very sensitive to the properties and relative proportions of matrix and reinforcement in the composite (usually expressed as the volume fraction of the reinforcement v_f) and the orientation of the reinforcement to the axis of loading.

For instance, the longitudinal Young's modulus E_L (the tensile modulus in the direction of the fibres in a unidirectional composite) is given by the rule of mixtures

$$E_L = E_f v_f + E_m (1 - v_f),$$

where E_f and E_m are the fibre and matrix moduli, respectively and v_f is the volume fraction. This rule is well-obeyed experimentally [see Fig. 7 and Adams and Bacon (1973a) and Adams and Short (1973)], and may be used as a check on any parameter provided the others are known. This relationship was derived for normal axial loading (tension or compression) but also applies in flexure, provided that shear effects can be neglected. In torsion (longitudinal shear), the mechanical behaviour for unidirectional composites is matrix dominated, but, again, it is possible to use vibrational measures of the shear modulus for material assessment (Adams and Bacon, 1973a).

The main sources of internal damping in a composite material arise from microplastic or viscoelastic phenomena associated with the matrix and relative slipping at the interface between the matrix and the reinforcement. Thus, excluding the contribution from any cracks and disbonds, the internal damping of the composite will be influenced by the volume fraction, the size of the inclusions (particle size, fibre diameter, etc.), the orientation of the reinforcing material to the axis of loading and the surface treatment of the reinforcement. In addition, loading and environmental factors such as amplitude, frequency and temperature may affect the measured damping values.

Composites are normally used in the form of laminates in which the fibres in one layer are all parallel, but they may be orientated at some angle θ to the next layer. Ni and Adams (1984) showed that it is possible to predict the damping and in-plane tensile modulus of beams cut at various

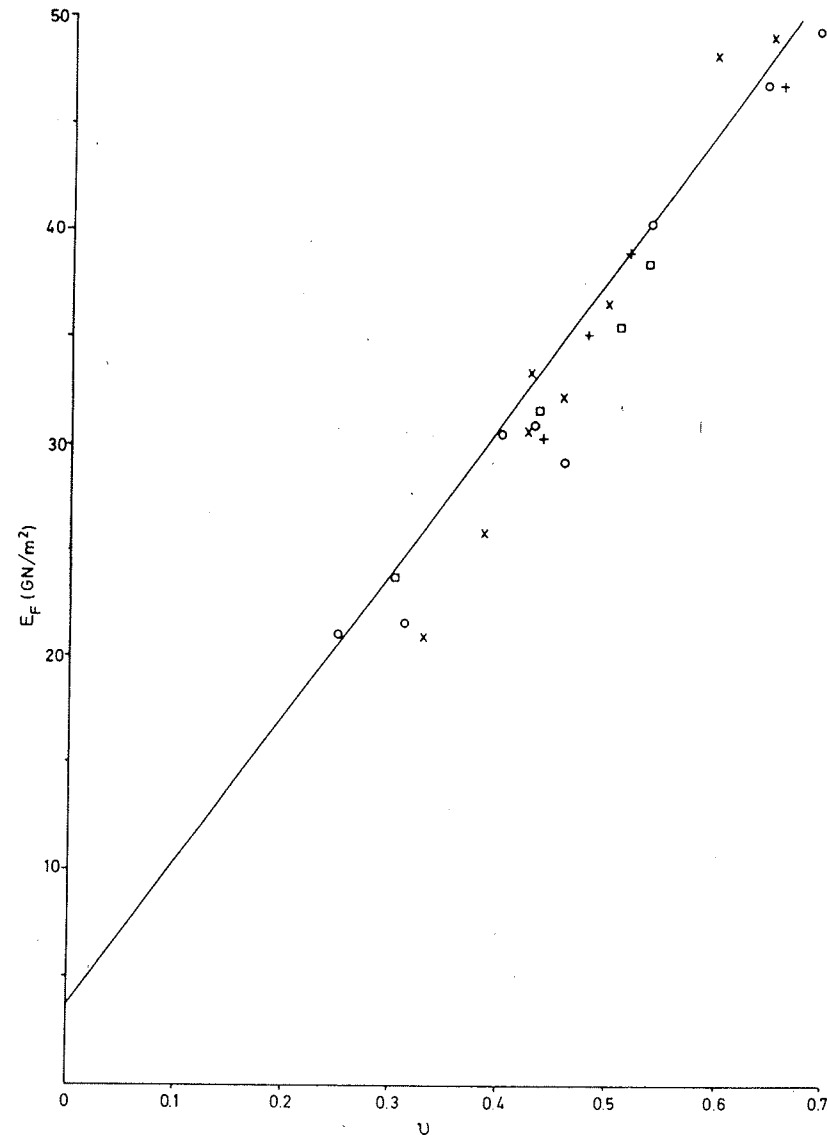


FIG. 7. Variation of flexural Young's modulus E_F with volume fraction v for glass fibres in polyester resin. Solid line is the law of mixtures. For the data plotted d equals 10 (□), 20 (+), 30 (O) and 50 (x) μm . [From Adams and Short (1973).]

could this

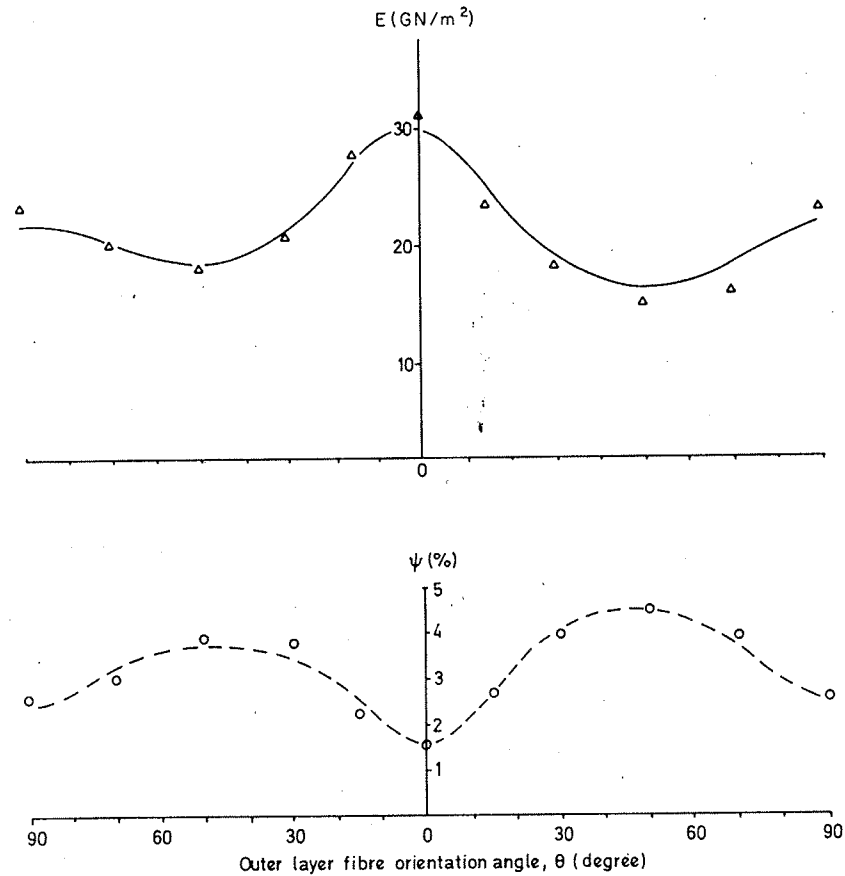


FIG. 8. Variation of flexural modulus E , and damping ψ , with outer layer fibre orientation angle θ , for specimens cut at angle θ to 0° layer (0° , 90° , 45° , -45°)s in glass/DX-210. — theoretical E ; Δ experimental E ; --- theoretical ψ ; \circ experimental ψ . [From Ni and Adams, (1984).]

angles from a laminate. Measurements made in flexural vibration on such beams cut from a carefully prepared GFRP plate (0° , 90° , 45° , -45° , -45° , 45° , 90° , 0°) confirmed the theoretical predictions (Fig. 8). These results indicate the potential of vibration measurements for the quality control of composite materials. Some applications on real components are discussed in sections V and VI.

C. Effect of cracks and other damage on the damping and modulus

Consider the cracks shown in Fig. 9. Depending on whether the crack is normally open or closed, and in which direction the loads are applied, the effect of the crack will show a marked difference. For instance, when shear loading A is applied to crack (a), the relative motion between the sides of the crack will result in energy dissipation through friction, while the open crack (b) will not. However, both will exhibit a locally reduced stiffness, since even the frictional forces in crack (a) will provide small restraint compared with that of an otherwise intact crystal lattice. When tensile loading B is applied to either crack, little energy dissipation will occur, but there will be a local reduction in stiffness. Compressive loading C will close crack (a) and tend to close (b), but whether closure occurs in the latter case is dependent on the load and the initial crack size.

In general, cracks tend to be open in the middle and closed at the ends, as shown in Fig. 9(c). Also, the loading D may be at some angle θ to the plane of the crack, resulting in both shear, tensile and compressive forces. Sliding friction will occur at the crack ends and larger normal motion at the middle, leading to both a local reduction in stiffness and a local dissipation of energy.

There are, of course, many forms of damage other than simple cracks. For instance, the material may have been subject to microplastic strain by creep or fatigue. Alternatively, some form of environmental attack may have taken place, such as by water or solvents in polymers, or by hydrogen embrittlement, in metals, or by nuclear radiation in any material. Under these circumstances, the defective zone may be local or general in the component.

1. Metals

Lazan (1968) showed that for most materials subject to cyclic stressing, once the cyclic stress sensitivity limit (CSSL) had been exceeded, the

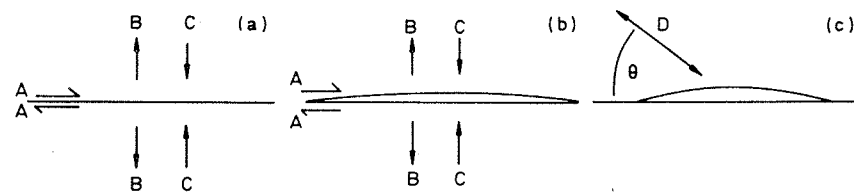


FIG. 9. Cracks under static and dynamic loads: (a) zero volume crack, both sides touching; (b) normally open crack or void; (c) part open, part closed crack.

damping would increase monotonically with the number of cycles; the greater the stress, the greater is the rate of damping increase. Since, for steels, the CSSL is usually less than the fatigue limit, this is a means of determining the onset of fatigue.

Sumner and Entwistle (1959) showed that torsional stressing in excess of the CSSL leads to an irreversible change in the magnetomechanical damping of carbon steels. Adams (1972a) showed that for a 0.52% C steel (in which the magnetomechanical damping had been suppressed by applying a saturating magnetic field), damage induced by exceeding the CSSL could be detected at lower cyclic stresses. Referring to Fig. 10, the damping-stress curve of the virgin material follows line *ab*, which is essentially independent of amplitude for increasing and decreasing cyclic stress. The CSSL was then exceeded (at about 240 MN m^{-2}) and, on retesting, the

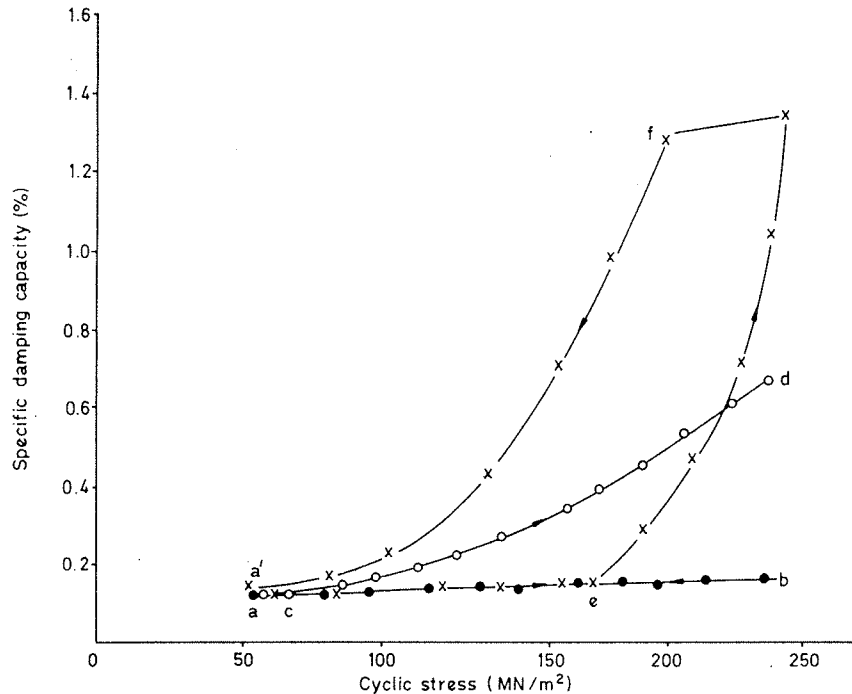


FIG. 10. Damping versus stress and stress history. Annealed 0.52% C steel magnetized to saturation. Before exceeding σ_L (*ab*), within one day of exceeding σ_L (*acd*) and 55 days after exceeding σ_L (*aef*). ●, increasing and decreasing stress; ○, increasing stress; ×, increasing and decreasing stress. [From Adams (1972a). With permission from *J. Sound Vibration* 23 (2), 199-216. Copyright 1972 by Academic Press Inc. (London) Ltd.]

line *acd* was followed. The CSSL had therefore been reduced from greater than *b* to about 70 MN m^{-2} . Ageing the material for 55 days at room temperature allowed the CSSL to increase to about 176 MN m^{-2} but, once this was exceeded, the effective value was again reduced to about 70 MN m^{-2} .

Briefly, the explanation for this is as follows. At stresses greater than the CSSL, dislocations are broken away from their pinning points so that

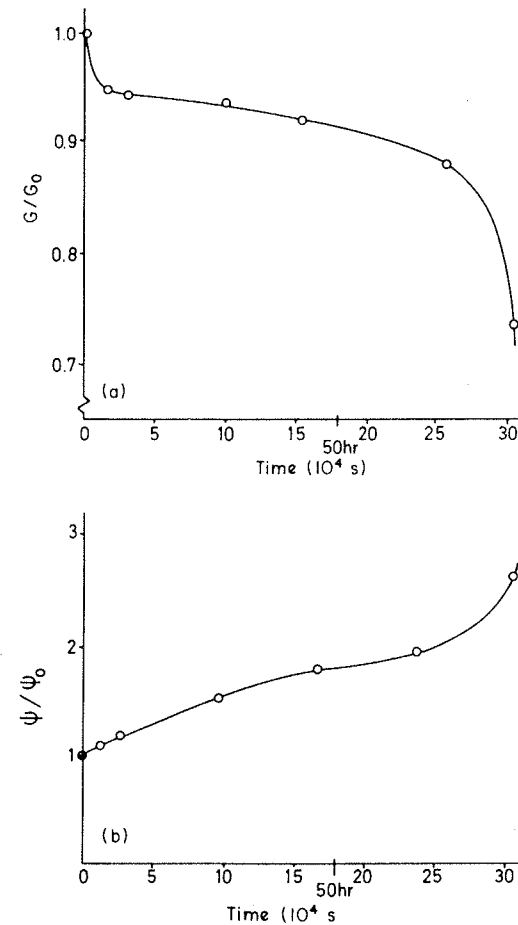


FIG. 11. Effect on unidirectionally reinforced GFRP of exposure to steam. (a) Change of shear modulus ratio with time; (b) change of damping modulus ratio with time. [From Adams (1976).]

a smaller stress is then required to move them. Subsequent testing at a lower stress will therefore show higher damping (curve *efa'*). As the stress is reduced further, it is unable to move even unpinned dislocations, so the damping falls to the original level. The 55-day ageing process allowed some migration of interstitials to the dislocations, which were then repinned. Low-temperature annealing for an hour at 200°C is known greatly to accelerate this process. Thus, relatively low amplitude damping measurements can be used to indicate fatigue damage in materials.

2. Composites

In composites, a common cause of trouble is attack by aggressive environments, such as steam or solvents. For example, when cylindrical, unidirectional specimens of carbon or glass reinforced plastic (CFRP and GFRP, respectively) are subjected to steam or boiling water, the matrix is softened (Adams, 1976). Figure 11 shows that the shear modulus reduces with exposure, while the damping increases. Both of these parameters are expressed as a proportion of the modulus and damping of the virgin material.

Damage induced by torsional fatigue occurs in the matrix and at the fibre-matrix interface but rarely within the fibres. Adams and co-workers (Adams *et al.*, 1973, 1974a, 1974b) showed that the damping increases with fatigue history while the modulus decreases, as shown in Fig. 12. Work in the same laboratory showed that static loading to produce longitudinal shear cracks has a similar effect on damping and modulus. Guild and Adams (1981) have shown that cracks through the fibres in a 0° GFRP beam can also be detected by damping measurements.

Thus, it is probable that most types of stress-induced damage in fibrous composites are manifest by local or global (depending on the nature of the damage) reductions in stiffness and increases in damping.

III. VIBRATION CHARACTERISTICS OF STRUCTURES

A. Single degree of freedom system

The simplest form of vibrating structure is the single degree of freedom spring-mass system shown in Fig. 13. If the material of the spring exhibits a hysteresis loop as discussed in section II, the system may approximately be modelled by representing the stiffness as a complex quantity,

$$k^* = k(1 + i\eta), \quad (1)$$

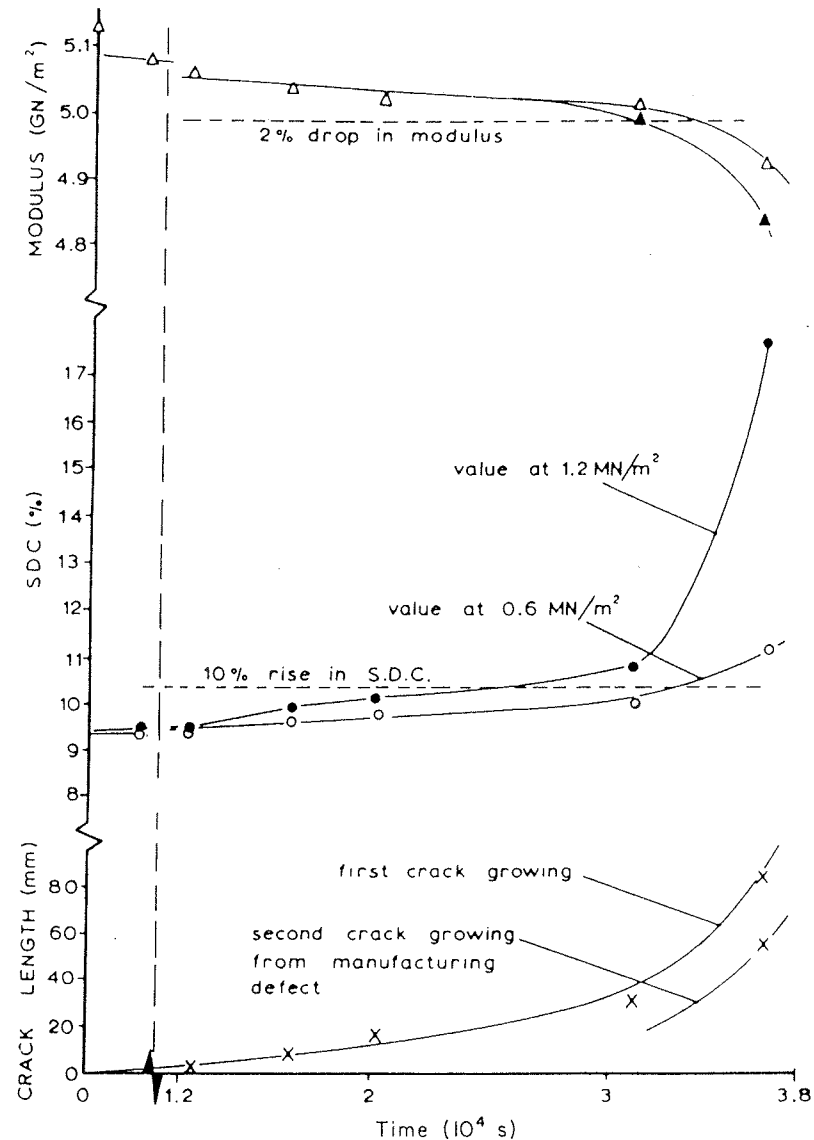


FIG. 12. Variation of damping, dynamic modulus and crack length with fatigue history of a longitudinally reinforced glass fibre in epoxy resin specimen. [From Adams *et al.* (1974). Reprinted with permission, from *ASTM STP 580*. Copyright ASTM, 1916 Race Street, Philadelphia, Pennsylvania 19103.]

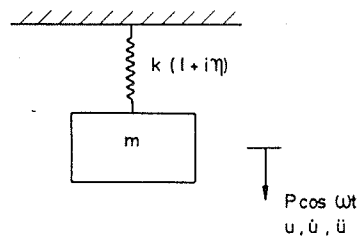


FIG. 13. Single degree of freedom system with hysteretic damping in forced vibration.

where η is the loss factor of the material. The energy dissipation per cycle is given by

$$\Delta W = \pi \eta k u_0^2 \quad (2)$$

where u_0 is the cyclic displacement amplitude.

If the system shown in Fig. 13 is subjected to a harmonic exciting force $P_0 \cos \omega t$, the displacement response will be given by $u = u_0 \cos(\omega t - \phi)$ where

$$|u_0/P_0| = 1/k[(1-r^2)^2 + \eta^2]^{1/2} \quad (3)$$

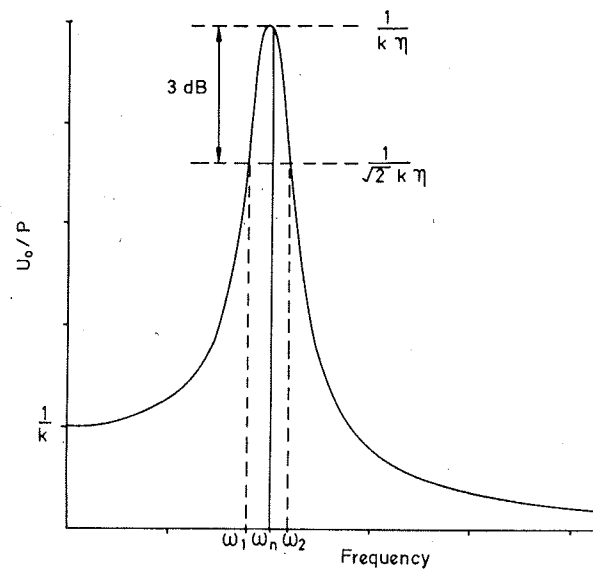


FIG. 14. Frequency response function for system of Fig. 13.

where $r = \omega/\omega_n$ is the frequency ratio, $\omega = 2\pi f$ the frequency in radians per second, $\omega_n = \sqrt{k/m}$ the natural frequency and m the mass. The phase angle ϕ is given by

$$\tan \phi = \eta/(1-r^2). \quad (4)$$

The maximum response occurs at the natural frequency ($r = 1$) and is given by

$$|u_0/P_0|_{\max} = 1/k\eta. \quad (5)$$

A typical frequency response function, $|u_0/P_0|$ versus frequency, is shown in Fig. 14. If the damping is increased, the resonant frequency is not changed but the maximum response is reduced. If the phase angle between force and response is also measured, the results may be presented in a Nyquist plot. At any frequency, ω the response u/P is plotted as a vector of length $|u_0/P_0|$ at an angle ϕ to the reference axis. This results in a circular locus as shown in Fig. 15 whose diameter is inversely proportional to the damping factor η .

More complicated structures can often be represented by a series of masses and springs, as shown in Fig. 16.

Frequency response information is often presented in terms of the impedance, which is defined as

$$Z = P_0/v_0, \quad (6)$$

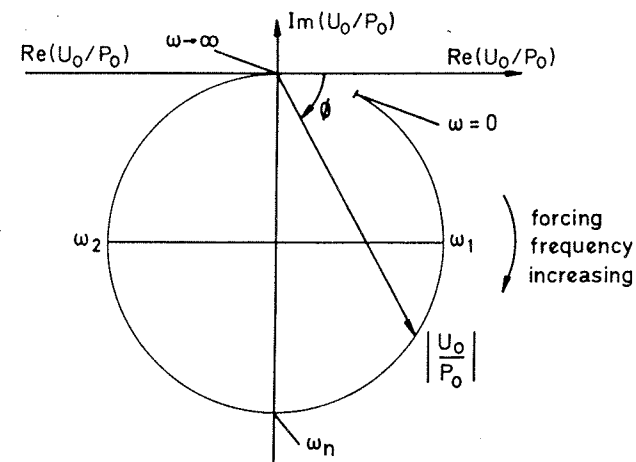


FIG. 15. Nyquist plot of frequency response function of system shown in Fig. 13, where ω_n is natural frequency and ω_1 and ω_2 are half-power points.

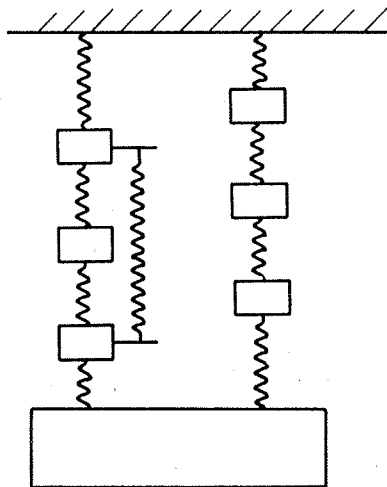


FIG. 16. Multi-degree of freedom system.

where v_0 is the velocity amplitude corresponding to a harmonic force of amplitude P_0 . For harmonic motion,

$$v_0 = \omega u_0, \quad (7)$$

so

$$Z = P_0 / \omega u_0. \quad (8)$$

Hence, resonances correspond to minima of an impedance versus frequency plot.

B. Continuous structures

The system discussed in the preceding section has only one degree of freedom and so has only one mode of vibration. Therefore the frequency response curve shows a single resonant peak. Continuous structures such as beams, plates and shells can vibrate in different ways (for example, axial, torsional and flexural vibration of a beam or shaft), and each type of vibration theoretically has an infinite number of modes. Therefore the frequency response curve of a continuous structure has many resonant peaks as shown in Fig. 17. However, around each peak, the motion is dominated by a single mode and so the response may be regarded as the sum of a series of single degree of freedom responses. This concept can be used in the measurement of the properties of each mode as discussed in section IV.

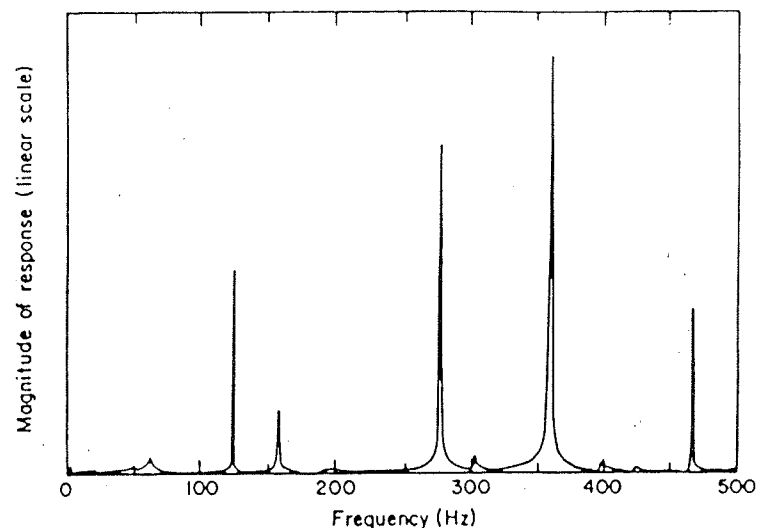


FIG. 17. Frequency response of rectangular aluminium plate. [From Cawley and Adams (1979d). With permission from *J. Sound Vibration* 64 (1), 123-132. Copyright 1979 by Academic Press Inc. (London) Ltd.]

The simplest case is the uniform bar in axial vibration for which the axial displacement u of a section at distance x from one end is governed by the equation

$$c^2 \partial^2 u / \partial x^2 = \partial^2 u / \partial t^2, \quad (9)$$

where c is the velocity of extensional waves (sound waves) and equals $\sqrt{E/\rho}$ where E is Young's modulus and ρ is the density. The steady-state solution to this equation is of the form

$$u = (A \cos \alpha x + B \sin \alpha x)(C \cos \omega t + D \sin \omega t), \quad (10)$$

where A and B are constants determined by the spatial boundary conditions, C and D are constants determined by the time boundary conditions and $\alpha = \omega/c$. For a bar with free ends resonating in its fundamental (lowest) mode of vibration, we have

$$u = u_0 \cos(\pi x/l), \quad (11)$$

where u_0 is the cyclic displacement at $x = 0$ and l is the length of the bar. This defines the displacement *mode shape* and is shown in Fig. 18(a). Note that the displacement is plotted vertically for visual convenience even though the motion is parallel to the axis of the bar. *Nodes* occur where the displacement is zero.

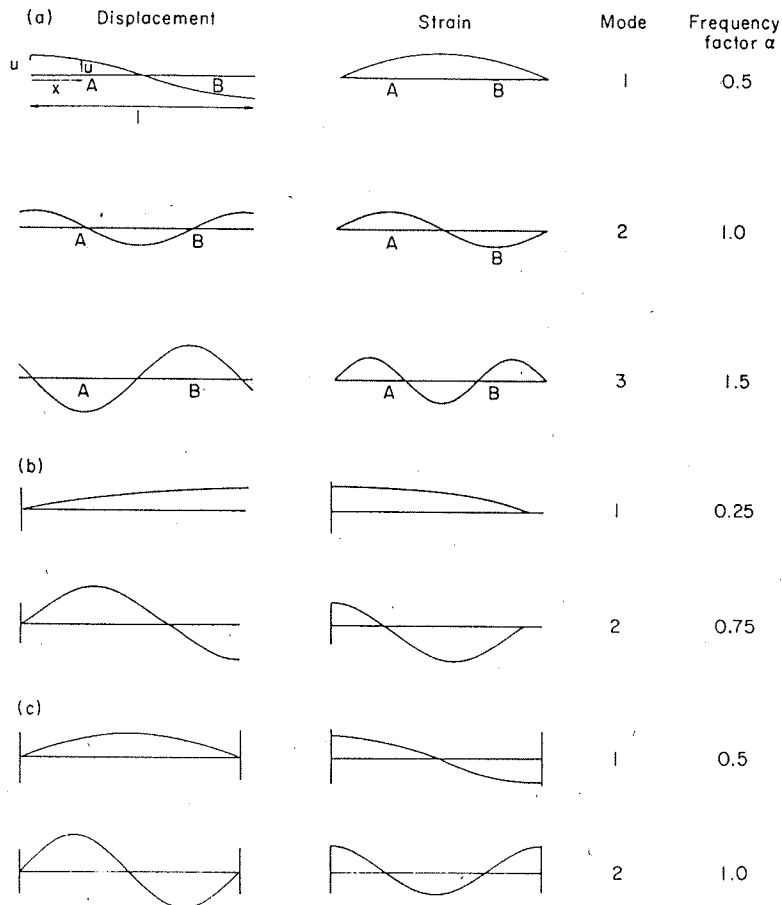


FIG. 18. Displacement and strain (stress) mode shapes for axial vibration of uniform bars (a) free-free, (b) fixed-free and (c) fixed-fixed. Frequency = $\alpha c/l$ Hz where $c = \sqrt{E/\rho}$, l is length, E Young's modulus and ρ density.

Sometimes, we are concerned with the cyclic stresses or strains. The strain ε is defined by $\varepsilon = \partial u/\partial x$ and the stress σ is defined by $\sigma = E\varepsilon = E \partial u/\partial x$ (assuming zero damping, although the error in most practical cases is negligible). In Fig. 18(b) we can see that the mode shapes for strain are quite different from those for displacement. For the first free-free mode, differentiation gives

$$\varepsilon = \partial u/\partial x = -(\pi u_0/l) \sin(\pi x/l). \quad (12)$$

Similar equations to these can be used for torsional vibration but replacing E by G , the shear modulus.

A more common but more complicated case is that of flexure. Here, the differential equation governing the motion is

$$\rho a \partial^2 v/\partial t^2 = -EI \partial^4 v/\partial x^4, \quad (13)$$

where v is the displacement perpendicular to the plane of the beam, a the cross-sectional area, and I the second moment of area.

The steady-state solution is

$$v = (P \cos \alpha x + Q \sin \alpha x + R \cosh \alpha x + S \sinh \alpha x)(T \cos \omega t + U \sin \omega t), \quad (14)$$

where P , Q , R and S are constants governed by the spatial boundary conditions and

$$\alpha^4 = \rho a \omega^2/EI$$

Typical mode shapes and natural frequencies for free-free and fixed-free boundary conditions are shown in Fig. 19. The fixed-free condition is similar to the situation experienced by a tuning fork or a turbine blade.

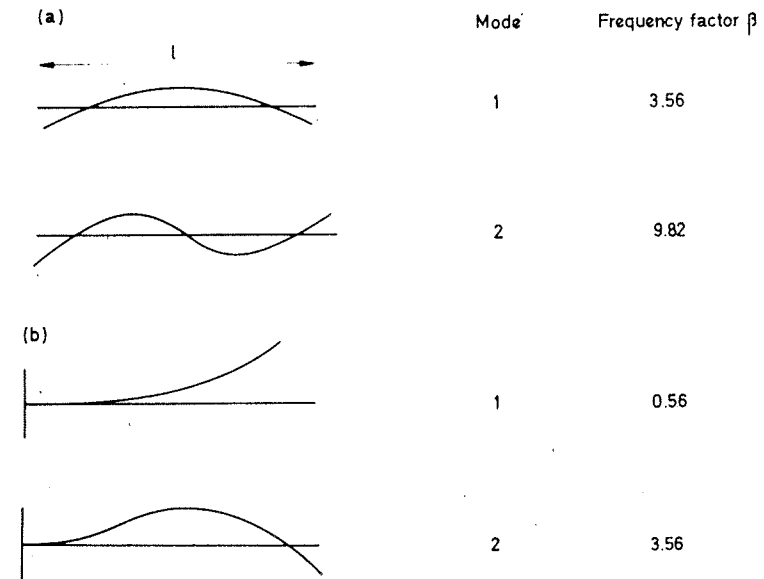
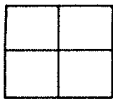

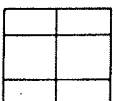
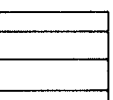
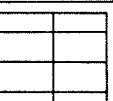
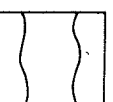


FIG. 19. Flexural mode shapes of beams (a) free-free and (b) clamped-free (cantilever). Frequency = $\beta/l^2 \sqrt{EI/\rho a}$ Hz where l is length, I 2nd moment of cross section, E Young's modulus, a cross-sectional area and ρ density.

The mode shapes of plates and shells are more complex. For example, Fig. 20 shows the nodal line patterns and corresponding natural frequencies and specific damping ratios for a hybrid carbon and glass fibre reinforced plastic plate.

In some cases, one section or member may be more flexible than its surroundings and this may appear to vibrate almost independently from

No.	Freq (Hz)	Mode Shape	SDC (%)
1	59.49 (60.17)		7.15 (7.1)
2	87.35 (86.30)		4.66 (5.1)
3	149.58 (149.3)		6.27 (6.4)
4	242.0 (237.3)		4.64 (5.1)
5	305.44 (299.95)		5.52 (6.9)
6	342.14 (335.03)		0.49 (0.78)

Outer layer fibre direction →

FIG. 20. Predicted and measured natural frequencies and specific damping capacities of various modes of vibration of a hybrid carbon-glass FRP plate. Experimental values in brackets.

the rest of the structure. This is rather like clamping a cantilever to a massive block which is in turn attached to the earth. The cantilever has clearly defined frequencies, but the block is not rigid nor of infinite mass, and so it too will respond to the cantilever vibration and so, to an even lesser extent, will the earth's crust.

C. Effect of defects

1. Cracks

If a structure is defective, as referred to in section II, there is a change in the stiffness and damping of the structure in the region of the defect. Usually, the stiffness decreases and the damping increases if the defect is in the form of a crack or series of cracks (micro or macro), or if the matrix of a fibrous composite has been attacked environmentally such as by steam or some other active agent. A reduction in stiffness implies a reduction in the structural natural frequencies and hence there is the possibility of using natural frequency measurements as a nondestructive test. Similarly, the damping of the different modes of vibration may be measured.

2. Effect of dimensional and similar changes

The expressions for the flexural natural frequencies of a beam shown on Fig. 19 indicate that natural frequencies are very sensitive to dimensional changes and so natural frequency measurements may be used to check that a component is within the prescribed tolerances.

In fibrous composites, the omission or incorrect orientation of a ply layer may be difficult to ascertain without destroying the structure. However, such a defective structure will have changes in its natural frequencies compared with a perfect one and a vibration technique may therefore be used to obtain a quick indication of the structural condition. In structures such as filament wound tubes, incorrect fibre winding, the omission of a tape helix and incorrect cure also affect natural frequencies and so may be detected.

IV. METHODS OF MEASURING THE NATURAL FREQUENCIES AND DAMPING CHARACTERISTICS OF SPECIMENS AND STRUCTURES

Natural frequencies and damping values may be determined by either steady-state or transient test techniques. The advent of cheap and powerful microprocessors has led to a change from steady-state to transient testing in recent years and the resultant decrease in testing time has made

vibration methods more attractive for NDT. The principles of both testing methods are discussed below.

A. Steady-state methods

The traditional method of measuring the natural frequencies and corresponding damping factors of a structure is to apply sinusoidal excitation to the structure via a shaker and measure the ratio of the response amplitude to the input force as the frequency of excitation is varied through the range of interest. The frequency response curve may then be plotted. The technique has been described in detail by, for example, Ewins (1976).

When accurate damping measurements are required, great care must be taken to ensure that a minimum of extraneous damping is introduced by the excitation system and the supports for the structure. This can involve, for example, supporting the structure at the nodes of the vibration mode under consideration so that no friction damping is introduced by the structure sliding over the supports.

Referring to the response curve shown in Fig. 14, the resonant frequency is determined simply by identifying the frequency at which the response is a maximum and the damping may be found by locating the half-power points, that is the frequencies ω_1 and ω_2 at which the response is $1/\sqrt{2}$ times (3 dB down from) its maximum value. It may readily be shown that the specific damping capacity is given by

$$\psi = 2\pi(\omega_2 - \omega_1)/\omega_n \quad (15)$$

Unfortunately, the use of this equation assumes that the damping is not a function of amplitude, which is often untrue for many materials. This leads to the case shown in Fig. 21(a). Several constant-damping curves A, B, C and D are shown such that $\psi_A < \psi_B < \psi_C < \psi_D$. If the system has a nonlinear damping–amplitude curve as shown in Fig. 21(b) then, at low amplitudes, the amplitude–frequency curve will follow resonance curve A. As the frequency increases, so does the amplitude and hence the damping, so that the response curve of the nonlinear system will leave curve A and move through B to C and thence to its maximum amplitude on curve D. As the frequency increases beyond the resonant point, the nonlinear response will drift towards curve A. The paradox is that if we measure the 3 dB points (at $u_D/\sqrt{2}$) we will get a value of $\Delta\omega'_D$ for the nonlinear curve, and $\Delta\omega_D$ if the damping had been constant at the value for curve D, the maximum attained. Then

$$\Delta\omega_D/\omega_n < \Delta\omega'_D/\omega_n \quad (16)$$

or

$$\psi_D < \psi'_D,$$

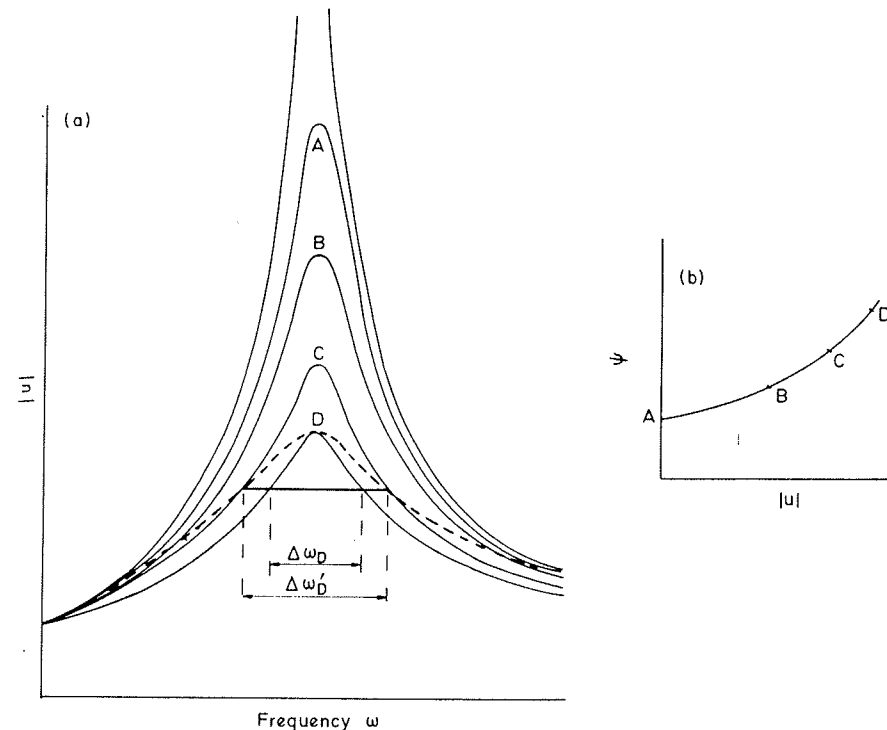


FIG. 21. Nonlinear damping curve shown (a) superimposed on a set of linear curves to illustrate the measurement error owing to amplitude-dependence of damping (b).

where ψ'_D is the apparent or measured value of the damping. Thus, although for the nonlinear system the true damping never exceeded ψ_D , the value measured from the amplitude–frequency curve will be larger than this. This is a most important point in measuring the damping of nonlinear systems, but is one which is rarely recognized.

One solution to this problem is to keep the amplitude constant at each frequency by varying the applied force as required via a feedback mechanism. If only a limited part of the resonance curve is used, this is practical and avoids the nonlinear damping–amplitude problem.

The frequency response information may also be plotted on a Nyquist diagram as shown in Fig. 15. The natural frequency is the frequency at which the rate of change of phase angle with frequency is a maximum (this procedure is more reliable than taking the resonant frequency to be the point at which the locus crosses the imaginary axis) and the half-power points may be found from a simple geometrical construction.

As discussed in section III, real structures have many modes of vibration and so the response curve is more complex than that shown in Fig. 14. However, provided the resonances are well spaced and the damping is reasonably light, the form of the frequency response around resonance is similar to that for a single degree of freedom system and the methods described above may be used to find the natural frequency and damping for each mode.

B. Transient methods

One of the simplest means of measuring the damping of a single degree of freedom system is to displace it, release it from rest and measure the rate at which the resulting vibration dies away. This is frequently expressed in terms of the logarithmic decrement δ defined as

$$\delta = \ln(u_n/u_{n+1}), \quad (17)$$

where u_n is the amplitude of the n th cycle and u_{n+1} is the amplitude of the next cycle. It may readily be shown that the specific damping capacity is related to the logarithmic decrement by

$$\psi = 2\delta. \quad (18)$$

The technique as described above is not easy to apply to continuous structures because it is very difficult to displace the structure in the mode shape of a particular mode of vibration. The obvious means of applying transient excitation to a structure is to tap it with a hammer. When a structure is given an impulse, it will oscillate in all its modes of vibration, the relative strengths of the different modes being dependent on the nature and position of the impulse. Thus the structural response is a function of the natural frequencies and damping of all the modes of the system.

Fast analogue-digital converters and digital transient capture equipment have become available which enable a transient signal to be stored digitally in a computer memory. This data can be processed to yield the logarithmic decrements of each mode, but a more powerful technique is available. Modern digital spectrum analysers contain a fast Fourier transform program by which the amplitude-time data can be converted to amplitude-frequency data. A full description of the mathematics of the method is beyond the scope of this chapter, but the reader who seeks more information is referred to the excellent book by Randall (1977).

Using this technique, the time record of the response of a structure to an impulse such as that shown in Fig. 22 may be converted to the corresponding frequency spectrum shown in Fig. 17. The natural frequencies of the test structures are readily identified from the maxima of the spec-

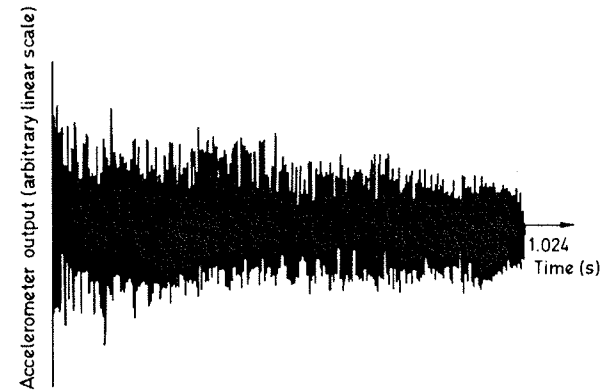


FIG. 22. Time record of acceleration response of rectangular aluminium plate to impact. Spectrum derived from this record shown in Fig. 17. [From Cawley and Adams (1979d). With permission from *J. Sound Vibration* 64 (1), 123-132. Copyright 1972 by Academic Press Inc. (London) Ltd.]

trum. The accuracy with which these frequencies can be defined is a function of the resolution of the frequency analyser.

By using a further technique called ZOOM analysis (also referred to as band selectable Fourier analysis), it is possible to concentrate the frequency data over a narrow range in the region of a resonant peak. It is then possible to determine the resonant frequency more accurately and also to determine the damping by the half-power bandwidth technique (provided that the damping is linear).

The measurement of structural natural frequencies by this technique is extremely quick; the testing time being about 1 sec and the apparatus is very simple and easy to set up. This makes the method very attractive for nondestructive testing. A block diagram of the testing configuration used to check the natural frequencies of filament wound CFRP tubes is shown in Fig. 23. Excitation was provided simply by tapping the top of the tube with a coin, the resulting vibration being detected by an accelerometer which was attached to the tube with wax. The signal from the accelerometer was passed to the spectrum analyser via a charge amplifier. Further savings in set-up time could be achieved by substituting a microphone for the accelerometer.

The calculation of modal damping values from transient test data takes a little longer than the determination of natural frequencies and more care is required in setting up the supports for the structure but the use of impulse excitation and digital signal processing is the most attractive damping measurement technique for nondestructive testing purposes. With modern analysers, the same experimental data can readily be pro-

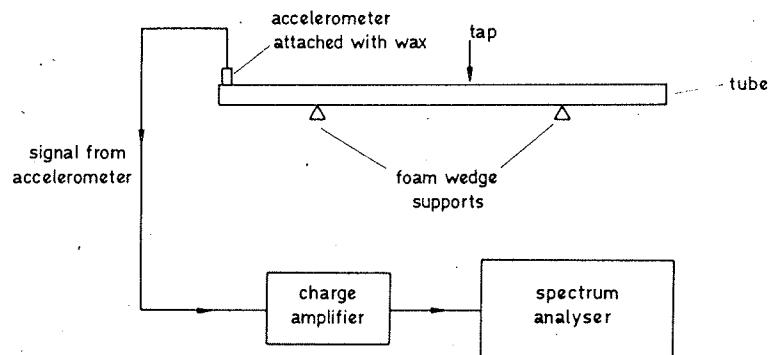


FIG. 23. Schematic diagram of apparatus used to check natural frequencies of filament wound CFRP tubes. [From Cawley *et al.* (1985).]

cessed to yield the natural frequencies and corresponding damping factors for several modes.

V. GLOBAL METHODS

A. Natural frequency measurements

1. Production quality control

Since natural frequencies are very sensitive to dimensions, their use for the detection of small cracks at the production stage is limited to components which are produced to strict dimensional tolerances. More generalized defects may be found in many components and structures. Frequency measurements can, of course, be used to check whether the dimensions are within the specification.

Natural frequency measurements have been used to check crankshafts and other iron castings by General Motors, Fiat and British Leyland (Spain *et al.*, 1964; Magistrali, 1975; Brown, 1973). The test is used to detect the degree of spheroidization in cast iron and the presence of internal defects. Magistrali (1975) says that the procedure permits a quick overall assessment of the integrity or otherwise of bulky parts where a thorough procedure of localized ultrasonic inspection would be too laborious and would be hampered by irregular coupling surfaces. Since these reports were written, the advent of relatively cheap spectrum analysers has meant that the cost of the equipment required and the testing time have been reduced considerably.

Adams and Vaughan (1981) developed a modulus parameter for assess-

ing the grade of a cast iron from its stress nonlinearity (see section II), thus removing the constraint of close dimensional consistency which is demanded by the usual (sonic modulus) tests. The effective modulus at different amplitude levels was obtained from natural frequency measurements.

The quality of grinding wheels can readily be assessed by natural frequency measurements (Peters *et al.*, 1969). The method is suitable for the determination of the hardness of both vitrified and resinoid wheels and gives a reliable indication of the behaviour of the grinding wheel under working conditions. Shen (1982) has recently produced a report on the technique and its implementation in the Grindo-Sonic system. A similar test has been used to test refractory linings in the Soviet Union (Konovlova *et al.*, 1973).

Cawley *et al.* (1985) have investigated the use of natural frequency measurements for the production quality control of fibre composites. Flexural vibration tests were carried out on a series of filament wound CFRP tubes, several of which had deliberately built-in defects. Some of the defective tubes had incorrect fibre volume fraction or winding angle while others had localized defects such as siliconized paper inserts and cut fibres. Figure 24 shows a graph of first mode natural frequency versus second mode frequency for all the tubes. The generalized defects, low-volume fraction and incorrect winding were readily detected. Until advances in production techniques improve the consistency of "good" tubes, small localized defects will not be found since they cannot be discriminated from the normal distribution of frequencies for "good" tubes. Lay-up errors in structures fabricated from pre-impregnated fibre sheet were also found. Similarly, it is likely that poor curing would be detected.

Lloyd *et al.* (1975) tested a batch of $152 \times 19 \times 7$ -mm steel bars, some of which had saw cuts of varying depth at a single section. They showed that natural frequency changes could be used to detect the damaged bars. Adams *et al.* (1978) showed that saw cuts and cracks have very similar effects on natural frequencies so these results were also applicable to cracks. Cawley (1985) has shown that natural frequency measurements provide a very quick and effective means of detecting cracks in mass-produced components fabricated from powder metal.

Davis and Dunn (1974) have used natural frequency measurements to check the integrity of concrete piles. Lilley *et al.* (1982) have extended this work to predict the location and severity of the defect using a technique similar to that developed by Cawley and Adams (1979a,b,c), which is discussed in section V.A.2. Both bulb and necking defects were located successfully, the maximum error in defect location being 3% while the maximum error in the length of the defect was 5%.

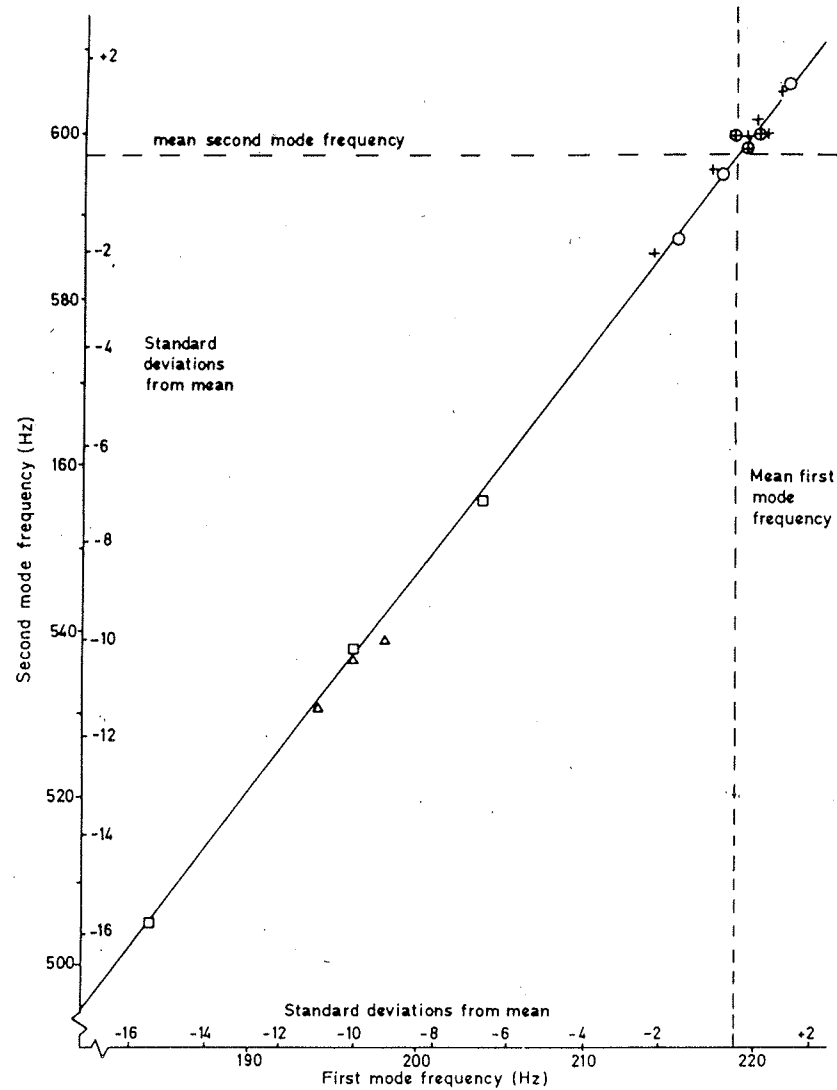


FIG. 24. First and second mode flexural frequencies for good and faulty filament wound CFRP tubes. +, good tube ($\pm 45^\circ$); O, tube with siliconised paper inserts ($\pm 45^\circ$); \oplus , tube with cut fibres ($\pm 45^\circ$); \triangle , misaligned tube ($\pm 50^\circ$); \square , tube with low fibre volume fraction ($\pm 45^\circ$). (From Cawley *et al.* (1985).)

2. In-service tests

Natural frequency measurements may also be used as an in-service test, measurements after a period of service being compared with a base line taken on the *same* component. The use of a baseline on the same component means that the effect of dimensional variations across a production batch is removed so greater sensitivity to small defects may be expected. One-off components may also be inspected which is impossible at the production stage in the absence of a standard for comparison.

Savage and Hewlett (1978) have used natural frequency measurements to monitor crack growth in concrete beams and also to check repairs made using epoxide resin. They term the technique the Savage and Heierli resonant investigation method (SHRIMP) which has been registered as a trade-mark.

Chondros and Dimarogonas (1980) have shown that natural frequency measurements can be used to monitor crack growth in the weld at the root of a cantilever beam. Figure 25 shows the relationship between the measured first mode natural frequency ω_n and the crack depth α . These values are normalized to the natural frequency in the undamaged state ω_{n0} and the section depth h , respectively.

Nagy *et al.* (1978) and Dousis and Finch (1980) have investigated the use of natural frequency measurements for the in-service inspection of railway wheels. Since the storage of baseline data from each wheel was not practicable, they compared the natural frequencies of the two wheels on the same axle. This ensured that the degree of acceptable wear would be similar, though the sensitivity of the test would still be limited by the

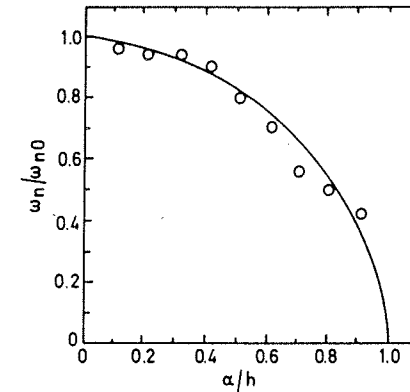


FIG. 25. Diagram relating crack depth α to the change of natural frequency of vibration ω_n . [From Chondros and Dimarogonas (1980). With permission from *J. Sound Vibration* 69, 531-538. Copyright 1980 by Academic Press Inc. (London) Ltd.]

dimensional consistency across a production batch. The wheels were excited by an automatic hammer as the train moved slowly past the test site, the resultant vibration being detected by a microphone. It was demonstrated that "plate" cracks in the web of the wheel and thermal cracks in the rim could reliably be detected.

Natural frequency measurements may also be used to locate the position of damage within a structure. The stress distribution through a vibrating structure is nonuniform and is different for each natural frequency (mode). This means that any localized damage affects each mode differently, depending on the particular location of the damage. The damage may be modelled as a local decrease in the stiffness of the structure, and so, if it is situated at a point of zero stress in a given mode, it will have no effect on the natural frequency of that mode. On the other hand, if it is at a point of maximum stress, it will have the greatest effect.

Consider, for example, the first three axial modes of a uniform, free-free bar, whose stress distributions are sketched in Fig. 18. Damage at the middle of the bar would have a negligible effect on the second mode but would induce a maximum change in the natural frequencies of the first and third modes. However, if the damage were situated at site A, it would have a smaller effect on the first and third modes but would cause a relatively large change in the second mode frequency. It would therefore be possible to use measurements of the changes in the natural frequencies of the bar to locate the position of the damage.

Owing to symmetry, damage at site B would have an identical effect to damage at site A so the two sites could not be distinguished by this simple test. If, however, the bar were asymmetrical due to, for example, the addition of a mass at one end, it would be possible to define the damage site uniquely. This example used axial vibration in a very simple structure. The technique is, however, readily generalizable to other types of vibration and to more complex structures.

The location of the damage site requires the computation of the relative effect on several modes of damage at different sites within the structure. The experimentally measured changes may then be compared with the theoretically calculated changes for damage at different sites and the position of the damage deduced. The effect of damage may be determined by modelling the damage as a local decrease in the stiffness of the structure and carrying out a dynamic analysis of the system. Since the effect of damage is dependent on the stress distribution, which is in turn dependent on the mode shapes, the requirement of the dynamic analysis is that a reasonable approximation to the mode shapes be obtained. The dynamic analysis may be carried out by any convenient technique.

The authors have carried out extensive tests on the method (Adams *et al.*, 1978; Cawley and Adams 1979a, 1979b, 1979c). Over forty tests were carried out on one- and two-dimensional structures with a variety of forms of damage including holes, saw cuts, fatigue cracks, crushing, impact damage and local heating. All these forms of damage were successfully detected and located by comparing the natural frequencies measured before and after damage. An indication of the severity of the damage was also obtained. The results were presented in the form of a damage location chart which gives a measure of the probability of damage being at a given location. A value of 100 indicates the most probable site, lower values representing decreasing probabilities.

One series of tests was carried out on an automobile camshaft. Although this is a highly nonuniform structure, for the purposes of the damage location program it was found to be sufficiently accurate to model the shaft as a uniform, straight bar. This test showed that it is unnecessary to expend large amounts of effort and computer time in producing an accurate dynamic analysis. The camshaft was initially damaged by a single, shallow saw cut of depth 1.7 mm. This corresponded to a 3.5% reduction in the cross-sectional area of that section of the bar. The damage was successfully detected and located by the vibration measurements. The location chart produced for an 8% reduction in local area is shown in Fig. 26 together with a photograph of the camshaft. Because the shaft was modelled as a symmetrical structure, two possible sites are indicated.

Two structures were tested which are representative of the ways in which high-quality fibre reinforced materials are used in industry. One of these was a 610 × 520 × 10-mm honeycomb panel with CFRP facings which is used for floor panelling in aircraft. The panel was made asymmetrical by removing one corner and was damaged by heating one face with a

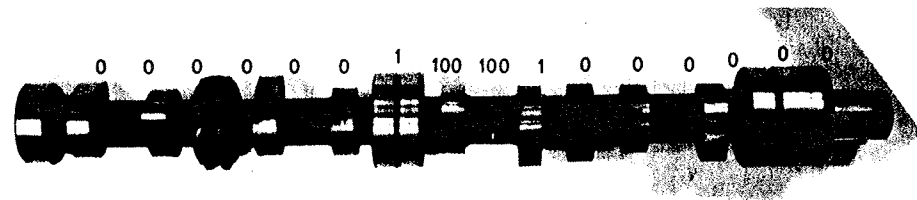


FIG. 26. Location chart for camshaft with saw cut damage (model crack). [From Cawley and Adams (1979c).]

gas flame. This produced a large blister on this face but the damage was invisible from the remote side. Figure 27 shows that the damage was successfully located.

Pye and Adams (1982) used the vibration technique not only to locate a defect in a bar, but also to predict the mode I stress intensity factor (as used in fracture mechanics). This technique has great promise for monitoring fatigue cracks via the local reduction in specimen stiffness associated with the crack propagation.

A similar technique has been used by the Central Electricity Generating Board (Mayes and Davies, 1976) to locate the position of transverse cracks in rotors. The location of the position of the crack was approached in a different manner to that described above. The effect of a transverse crack at various axial positions on the first four flexural natural frequencies of the rotor was derived in terms of the stress intensity factor for a

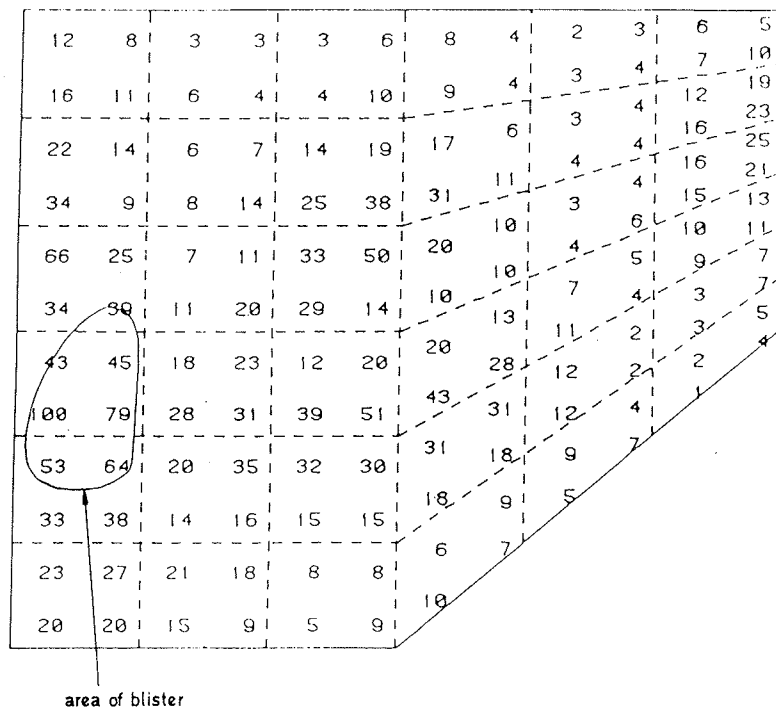


FIG. 27. Location chart for CFRP-skinned honeycomb sandwich panel damaged by local heating. [From Cawley and Adams (1979c).]

circumferentially notched bar and the experimentally determined mode shapes of the undamaged rotor.

Loland and MacKenzie (1974), Loland *et al.* (1975a, 1975b) and Loland and Dodds (1976) have applied the technique to off-shore oil rigs, using measurements of the natural frequencies of the framework obtained from the Fourier transform of the structural response to wave excitation. Their analysis did not attempt to locate the position of damage within a structural member but merely to predict whether a given member was fractured. There has been considerable interest in the technique in the oil industry and further discussion may be found in, for example, Coppolino and Rubin (1980) and Kenley and Dodds (1980).

The damage location predictions used in all the analyses described above have assumed a single damage site; extension of the technique to multiple sites has been considered by Al-Agha and Adams (1982).

B. Damping measurements

Structural damping is much less sensitive to dimensions than are the corresponding natural frequencies. Damping measurements may therefore be used as a production quality control test, even on components which are not produced to tight dimensional tolerances. They may also be used as an in-service test in the same manner as natural frequency measurements. Although damping tends to be more sensitive to damage than natural frequencies, it is much more difficult to measure accurately. In particular, care must be taken to minimize extraneous damping from, for example, the system supporting the component during the test.

The damping changes produced by a crack were discussed by Curtis and Lloyd (1980) who compared the waveform of the sound produced by cracked and uncracked teacups (see Fig. 28). This change is readily detected by ear and is the basis of the subjective test which has been used for many years in the crystal glass industry to detect cracked glasses. Lloyd *et al.* (1976) describe the testing of ceramic plates by this technique. Similar tests have been reported by Hoffman (1972), who also discussed the detection of poor joining on silver-soldered ammunition components by damping measurements.

Bray and Gianasso (1973) have investigated the damping of the small welded specimens shown in Fig. 29. After the damping measurements, the specimens were tested to destruction in a static tension machine. The relationship between the first mode loss factor η and the ultimate tensile load of the welded joint R is shown in Fig. 30. If a good joint is defined as one with an ultimate load greater than 800 kgf and the specimens with loss factor greater than 2.4×10^{-3} had been rejected, Fig. 30 may be split into

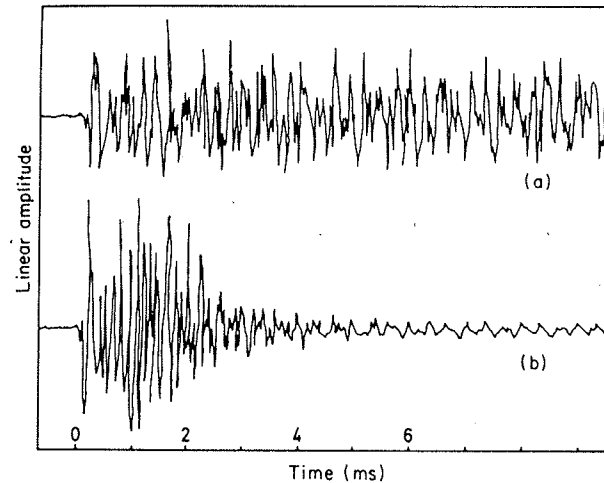


FIG. 28. Waveforms for (a) cracked and (b) uncracked cups after tap. [From Curtis and Lloyd (1980).]

four regions: I, good specimens—accepted, II, good specimens—rejected, III, defective specimens—rejected and IV, defective specimens—accepted. Specimens in regions II and IV have been wrongly classified. In this case, 2 out of 45 samples would have been incorrectly classified. It is likely that with improvements in the experimental technique and in the signal processing, these errors could be avoided.

Recent work at Imperial College on the clips used to secure railway tracks to the sleepers has shown that damping measurements may be used in the factory to check whether the clips have been correctly heat treated and whether any transverse cracks are present. Successful tests have also

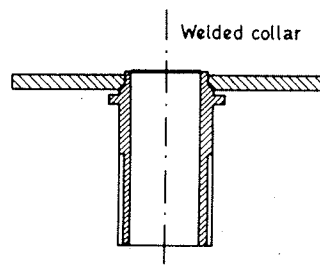


FIG. 29. Small welded component. [From Bray and Gianasso (1973).]

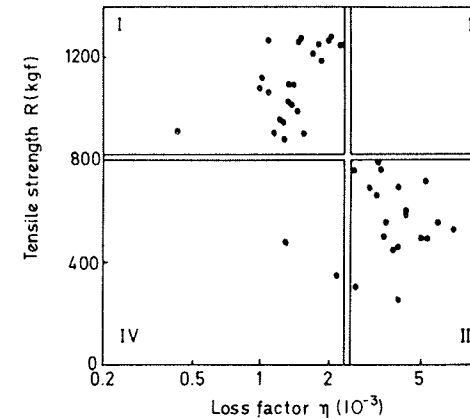


FIG. 30. Variation of ultimate tensile strength R with loss factor η for small welded components. [From Bray and Gianasso (1973).]

been carried out on copper brazed heat exchangers, poor brazing being detected through an increase in damping.

Daedalean Associates Inc. have produced a number of reports on the application of damping measurements to the nondestructive testing of a variety of structures (Fresch *et al.*, 1978; Hochrein and Yeager, 1978; Olver *et al.*, 1980; Yeager *et al.*, 1981). Their results show that fatigue cracks and other defects can be detected when the damping of a good component is low and when there is little damping introduced by the support system used. Their findings are similar to those described above. Daedalean also hoped to apply the technique to built-up structures. Unfortunately, unless the damping introduced at the structural joints is small, there is little prospect of success.

Schroeer *et al.* (1970) and Schroeer (1970) describe the development of the acoustic impact technique. The description of the method implies that damping measurements were used to detect cracks under fastener heads which are a major problem in the aircraft industry. It is highly unlikely that the testing arrangement described would achieve this since even good fasteners give a significant amount of friction damping and the apparatus shown would also add a considerable amount of extraneous damping to the system. This judgement is confirmed by Bickford *et al.* (1973). Schroeer also reports that disbonds in honeycomb panels can be detected by a similar technique. A study of the results reveals, however, that the detection of disbonds relies on applying the impact directly above the defective area. This means that the successful results were not based on

damping measurements but on the principles behind the local coin-tap test which is discussed in section VI.B.1.

C. Use of combined natural frequency and damping measurements

With modern signal processing equipment, it is becoming increasingly easy to measure both natural frequencies and damping in a single test. Both may be obtained by analysing the vibration waveform after an impact. This means that the advantages of the two may be combined. Twenty years ago, General Motors developed a modular system which could be used to make a combination of natural frequency and damping measurements (Spain *et al.*, 1964). Modern equipment could be used to perform a similar task, but would be more flexible.

Curtis and Lloyd (1980) have shown that the moments about the zero frequency axis of a spectrum computed from the response to an impact can provide a sensitive indication of damage. These moments contain a mixture of natural frequency and damping information and are a useful means of producing a single parameter on which to base a decision.

In further work on the in-service inspection of railway wheels which was discussed in section V.A.2, Finch and Thomford (1982) suggest that inspection reliability may be improved by including both damping and natural frequency measurements in the decision algorithm.

Hoffman and Addison (1974) used seven parameters computed from the response of a projectile to impulses at different points around its circumference to determine whether a band welded round the component was attached satisfactorily. This procedure improved the inspection reliability from the 85% achieved using damping measurements alone to approaching 100%. The test used was a hybrid of the global methods discussed in this section and the local coin-tap test.

D. Discussion of global methods

The global methods based on natural frequency and/or damping measurements discussed in this section have the major advantage that the whole component can be checked by measurements made at a single point. This means that very rapid testing is possible, particularly if a tap testing technique is employed. Not surprisingly, if a single point measurement is used to infer the quality of the whole component, the sensitivity of the technique tends to be lower than that obtained by local measurements such as ultrasonic inspection.

Cawley and Adams (1979c) showed that damage equivalent to a crack through 1% of the cross-sectional area of a one-dimensional structure at a single section could be detected by natural frequency measurements.

With two-dimensional structures, damage equivalent to the removal of about 0.1% of the area of the structure could be found. These values were obtained using base line measurements on the same component. The sensitivity to small defects is reduced by dimensional variations across a batch if the test is used at the production stage.

Kenley and Dodds (1980) concluded that natural frequency measurements made at a single point above the waterline on an oil rig would not detect damage less severe than the complete severing of one member of the framework. More detailed information could be obtained from local measurements as described in section VI.A.2. However, since these structures have a considerable amount of redundancy, the information gained from continuous monitoring above the waterline can be very valuable.

Damping is often more sensitive to damage than are natural frequencies and is insensitive to dimensional variations. However, it is much more difficult to measure accurately since care must be taken to minimize damping from the support system. Bickford *et al.* (1973) concluded that successful use of damping measurements on an aircraft structure with its many mechanical fasteners was a remote possibility. However, on single components, successful results can be obtained as discussed in section V.B. Work is currently in progress at Imperial College to determine the sensitivity of damping measurements to different types of defect. With practical testing techniques, this seems likely to be of the same order as that for natural frequency measurements, the best type of measurement depending on the particular application.

The reports in the literature together with the experience of the authors show that the global tests can serve a very valuable role, particularly in the production inspection of mass-produced components for which other techniques are impracticable because of the high testing times and therefore costs involved.

VI. LOCAL MEASUREMENTS

A. Excitation at a single point

Techniques in this category involve vibrating the test structure (usually at resonance) by applying an exciting force at a single point and measuring a local property of the structure in the particular mode of vibration at all the points of interest. If these measurements can be carried out by a scanning system, the test is potentially quick to carry out and, because local properties are being measured, it may be more sensitive than the global methods described earlier.

1. Vibrothermography

The presence of damage in fibre reinforced plastics results in the formation of cracks and crazes. When cyclic stresses are applied to a damaged composite material, relative motion takes place between the sides of the assorted cracks, resulting in the generation of heat (damping). The change in the overall level of damping in a structure is small for many forms of serious but localized damage, while the damping change in this small local area may be large. Various authors have used this technique, usually referred to as vibrothermography, for nondestructively examining structures. Usually, it is necessary that the structure has low thermal diffusivity to prevent the rapid conduction of heat from the damaged area. It is therefore of least application to metals (unless the dissipation rate is large) and of greatest application to materials such as GFRP. Carbon-based composites have markedly higher thermal conductivity than glass-based ones, and are not so easy to test.

This technique was originally applied to fatigue tests on composites in which the stresses were applied by large, servo-hydraulic machines (Reifsnider and Williams, 1974; Nevadunsky *et al.*, 1975). Henneke and Jones (1978) used ultrasonic excitation, while Pye and Adams (1981a, 1981b) and Reifsnider and Stinchcomb (1976) used resonant vibration. This latter technique is better termed *resonant vibrothermography*.

The advantage of using resonant vibration is that, for a given applied force, the stresses in the structure are greater than if the same force were applied at some other frequency, so that high-powered fatigue machines are not necessary.

Pye and Adams (1981b) used resonant vibration to detect shear cracks in unidirectional fibrous composites consisting of glass or carbon fibres in an epoxy resin matrix.

Pye and Adams (1981b) also considered the effect of the cyclic stress and frequency vibration on the temperature rises. They showed that, if other parameters remain constant, then the temperature difference ΔT between any two points of the structure is such that

$$\Delta T \propto \sigma^n f, \quad (19)$$

where σ is the peak cyclic stress, f the frequency of vibration, and the exponent n (usually greater than 2) a function of the damping-stress relationship in the region of the crack.

Using resonant vibration, it is often possible to use higher cyclic frequencies than can be obtained using servo-hydraulic machinery. Equation (19) shows that this will increase the sensitivity of the test, thus allowing easier detection of the damage or, alternatively, a reduction in the cyclic stress used.

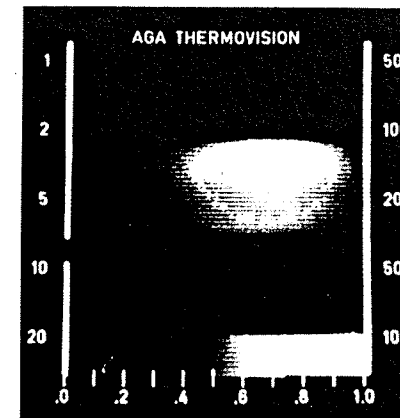


FIG. 31. Thermograph for GFRP tube using isotherm facility.

A thermograph showing damage in a $\pm 30^\circ$ filament wound GFRP tube is shown in Fig. 31.

2. Local amplitude measurement

Local damage in a structure tends to distort the vibration mode shapes. With the advent of laser holography systems, there has been an upsurge of interest in the exploitation of this effect in NDT (Erf, 1974). The technique involves vibrating the test structure at resonance and producing a time-averaged hologram of the motion (Campbell and McLachlan, 1979). The method has been particularly successful for detecting skin-core disbands in honeycomb panels. However, it is essential that the system be set up in a vibration-free environment. This means that it is only suitable for specialist applications.

The use of pulsed lasers makes it possible to use the technique in the presence of background vibration (Fagot *et al.*, 1980). In this case, the best results are obtained by using impulse excitation and producing the hologram from views taken a few microseconds apart as the pulse propagates through the structure. An example of the results obtained on an aluminium honeycomb panel containing two defects is shown in Fig. 32, the field observed being about 600 mm across. The technique is still under development and the equipment costs are high, but rapid inspection is possible and the method may prove cost-effective where large areas of structure are to be inspected.

A similar idea has been employed on multilayer structures in the Soviet Union (Lange and Moskovenko, 1978). They excited the structure over a

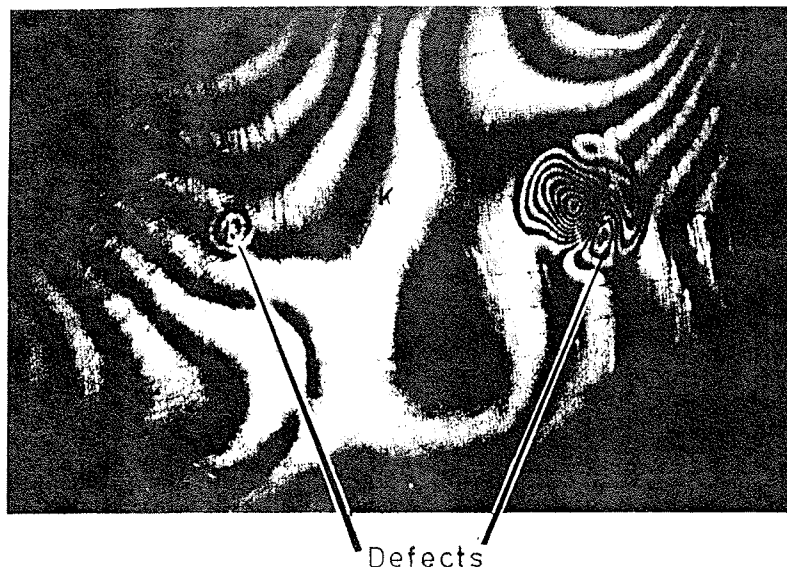


FIG. 32. Double exposure holographic view of defects in an aluminium honeycomb structure. [From Fagot *et al.* (1980).]

wide frequency band above the major structural resonances and used lycopodium powder sprinkled on the surface of the structure for detection. In defective zones, the amplitude was higher due to the membrane resonance effect discussed in section VI.B.3 and so the powder migrated away from these areas. The method is very quick and simple to apply but can only detect flaws to a depth of 3 to 5 mm. It also depends on there being a membrane resonance of the layer above the defect in the frequency range covered by the exciter. (See also section VI.B.3.)

Changes in mode shape have also been used to detect rot in wooden poles used for electricity pylons (Shaw, 1974). It is likely that natural frequency changes could also be used in this application.

Mode shape measurements have also been investigated as part of the development of continuous monitoring systems for oil rigs. Kenley and Dodds (1980) concluded that while natural frequency measurements using a single transducer could only detect the complete severing of one member of the framework, if accelerometers were placed at strategic points on members below the waterline, the flooding or half severance of members could be detected from local changes in the mode shapes. If the transduc-

ers were permanently attached, this did not require the use of divers, nor were a large number of transducers required.

B. Excitation at each test point

The methods described in this section all involve applying vibration excitation at each test point and measuring the input force and/or the vibration response at the same point. They are used for the detection of defects such as disbonds in adhesive joints, delaminations and voids in laminated structures and defective honeycomb constructions. These are all "planar" defects which result in one or more layers of the construction being separated from the base layer(s). The methods are not suitable for detecting transverse cracks (i.e., those running a direction normal to the surface).

The main advantage of these techniques over the higher frequency ultrasonic methods is that no coupling fluid is required between the transducer and the structure which results in more rapid and convenient testing. They are also easier to apply to honeycomb constructions.

1. The coin-tap test

As discussed earlier, the coin-tap test is one of the oldest methods of nondestructive inspection. It has been used regularly in the inspection of laminates and honeycomb constructions. Indeed Hagemaijer and Fassbender (1978) found that it could detect more types of defect in honeycomb constructions than any other technique except neutron radiography. Until the early 1980s, however, the technique has remained largely subjective and there has been considerable uncertainty about the physical principles behind it.

It should be stressed again that this test is quite different from the wheel-tap test discussed in section V, though the testing technique and subjective interpretation of the sound produced is similar in both cases. The wheel-tap test is a global test which investigates the whole test component from a tap applied at a single point, the difference between sound and defective components being detected from changes in the natural frequencies and damping. The coin-tap test will only find defects in the region of the tap, so it is necessary to tap each part of the structure under investigation.

The sound produced when a structure is tapped is mainly at the frequencies of the major structural modes of vibration. These modes are structural properties which are independent of the position of excitation. Therefore, if the same impulse is applied to a good area and to an adjacent defective area, the sound produced must be very similar. The difference

in the sound produced when good and defective areas are tapped must therefore be due to a change in the force input.

When a structure is struck with a hammer, the characteristics of the impact are dependent on the local impedance of the structure and on the hammer used. Damage such as an adhesive disbond results in a local decrease in structural stiffness and hence a change in the nature of the impact. The time history of the force applied by the hammer during the impact may be measured by incorporating a force transducer in the hammer. This technique is commonly used in structural dynamic testing (Peterson and Klosterman, 1978). Typical force-time histories from taps on sound and debonded areas of an adhesively bonded structure are shown in Fig. 33. The impact on the sound structure is more intense and of shorter duration than that on the damaged area, the impact duration on the sound structure being approximately 1 msec. The differences between the two impulses is more readily quantified if the frequency content of the force pulses is determined. This is achieved by carrying out a Fourier transform of the force-time records. The spectra derived from the force-time histories shown in Fig. 33 are given in Fig. 34. The impact on the damaged area has more energy at low frequencies but the energy content falls off

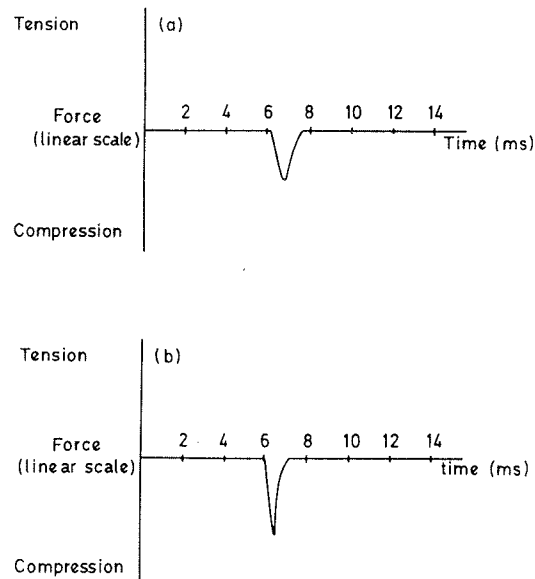


FIG. 33. Force-time records for impacts on (a) defective and (b) sound regions of adhesively bonded structure. [From Adams and Cawley (1983).]

rapidly with increasing frequency, while the impact on the sound area has a much lower rate of decrease of energy with frequency. This means that the impact on the defective area will not excite the higher structural modes as strongly as the impact on the good zone. The sound produced will therefore be at a lower frequency and the structure will sound "dead".

The testing technique therefore involves tapping the area of the structure to be tested with an automatic, instrumented hammer designed to give a single, reproducible impact and comparing the frequency spectrum of the impulse with that of an impulse from the same hammer on an area of the same type of structure which is known to be sound. Data from a sound structure would be stored in the testing instrument so that the instrument could carry out the comparison and give an immediate indication of the integrity of the area under test. This development is the subject of a patent application (Adams and Cawley, 1983).

2. The impedance method

The impedance method of nondestructive inspection has been used in the Soviet Union for almost thirty years (Lange and Moskovenko, 1978) and

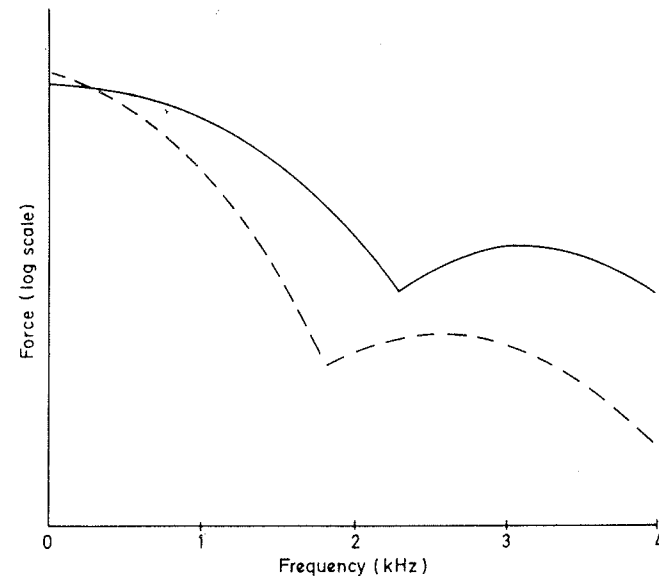


FIG. 34. Spectra of time records shown in Fig. 33 (—) sound and (---) defective area. [From Adams and Cawley (1983).]

its use in the West has now increased with the marketing of the Acoustic Flaw Detector, which is based on the Soviet design, by Inspection Instruments Limited. The technique uses measurements of the point impedance Z of a structure defined as

$$Z = P/v, \quad (20)$$

where P is the harmonic force input to the structure and v the resultant velocity of the structure at the same point. The measurements are carried out at a single frequency, typically between 1 and 10 kHz (Lange and Moskovenko, 1978). There has been considerable interest in the technique, particularly from the aerospace industry, but uncertainty about which physical parameters are measured and the relationship between these and the presence of defects has limited its application.

The impedance method seeks to detect areas of a structure where one or more layers are separated from the base layer(s) as shown in Fig. 35(a). A localized defect of this type has little effect on the overall dynamic properties of the structure. It has been shown (Cawley and Adams, 1979a, 1979c) that the change in mode shapes and structural natural frequencies produced by localized defects, while measurable, are in general small. Clearly, however, the local stiffness of the structure is significantly re-

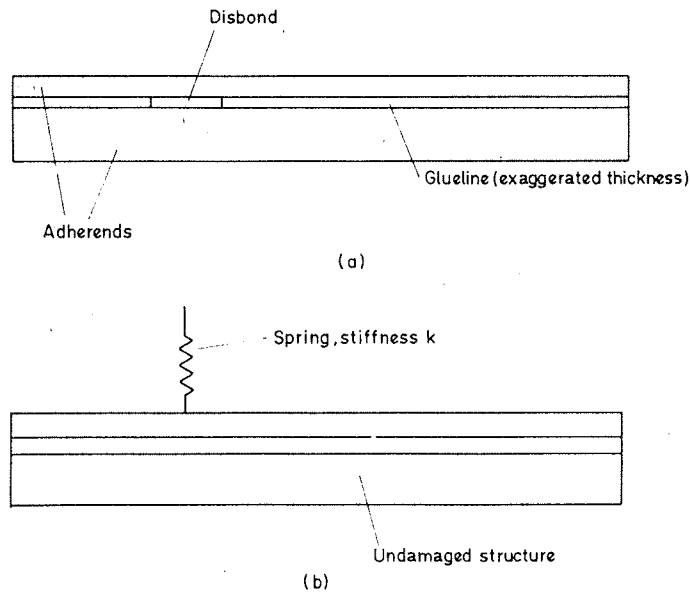


FIG. 35. Typical (a) defect and (b) mathematical model. [From Cawley (1984).]

duced. The defect may therefore be modelled as a spring, below which is the rest of the structure whose properties are unaltered, as shown in Fig. 35(b). The spring stiffness is given by the static stiffness of the layer(s) above the defect supported around the edges of the defect. The boundary condition is likely to be intermediate between simply supported and clamped.

The plate formed by the layer(s) above the defect can resonate. As the first resonant frequency, which is that of the membrane resonance discussed in section VI.B.3, is approached, the effective stiffness of the plate is reduced and the spring stiffness calculated from the static properties of the layer is no longer valid. However, for most defects, this frequency is outside the normal operating range of the instrument.

Cawley (1984) carried out a theoretical investigation of the impedance method and also measured the impedance changes produced by a number of defects. Figure 36 shows impedance–frequency curves taken on a laminate comprising an aluminium sheet 45 mm wide and 3.3 mm deep bonded to a 30-mm-deep steel beam. Two areas of the sheet, one 39 mm long and the other 17 mm long, were not coated with adhesive and so formed disbonds. Figure 36 shows that the defects can clearly be detected from impedance measurements.

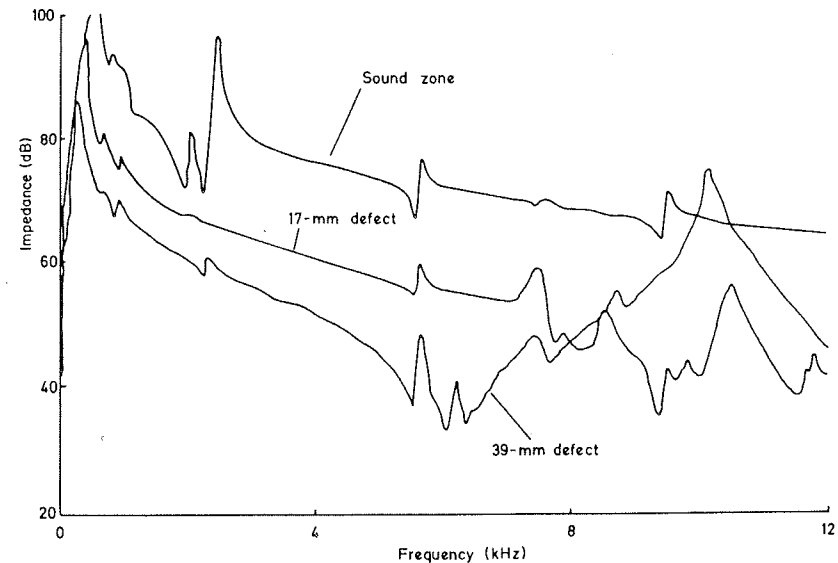


FIG. 36. Measured impedance–frequency curves for thick beam. [After Cawley (1984).]

These measurements were carried out using an impedance head (Ewins, 1976; Brownjohn *et al.*, 1980) cemented to the structure. For practical nondestructive testing, a dry point contact between the transducer and the structure is used. This contact has a finite stiffness (Lange and Teumin, 1971) so the spring stiffness in the model becomes the defect stiffness in series with the contact stiffness. The spring stiffness over a good area of the structure is the contact stiffness alone. It is important to keep the contact stiffness as high as possible as this is the major limitation on the sensitivity of the technique. The method is also most sensitive to defects between a thin top layer and a stiff base structure. Figure 37 shows the variation of minimum detectable defect diameter with depth for aluminium and carbon fibre reinforced plastic structures assuming a stiff base structure and a 3-dB reliability in impedance measurement (i.e., the impedance in a defective zone must be at least 3 dB lower than that in a sound zone if the defect is to be reliably detected). Typical values of contact stiffness were assumed, the technique being less sensitive for the CFRP facing because of a lower contact stiffness.

Problems have arisen with the systems currently employed both in the Soviet Union and the West because the transducers used, unlike the impedance head used in the tests reported by Cawley (1984), give an output which is a highly nonlinear function of the structural impedance and the simple physical interpretation which can be made of the results shown in Fig. 36 is lost.

3. Membrane resonance methods

It was shown in the previous section that the layer of material above a disbond or delamination may be modelled as a plate which is restrained around the defect edges. This plate can resonate, the first mode being the membrane resonance in which the motion is similar to that of a diaphragm.

As the frequency of vibration excitation approaches the membrane resonant frequency, the impedance of the system is reduced and the response amplitude obtained for a given force input increases. Therefore, at frequencies around the membrane resonance of the layer above a defect, the vibration response for a given force will be greater than that obtained in a sound region of the structure. Thus, a nondestructive test may be based on response measurements alone, assuming the input force to be approximately constant. Since the resonant amplification tends to be large (greater than a factor of 10, which is 20 dB), the controls on the size of the force need not be too sophisticated. The test is therefore potentially simpler than the impedance method discussed in the preceding section, which relies on measuring impedance changes of the order of 3 dB.

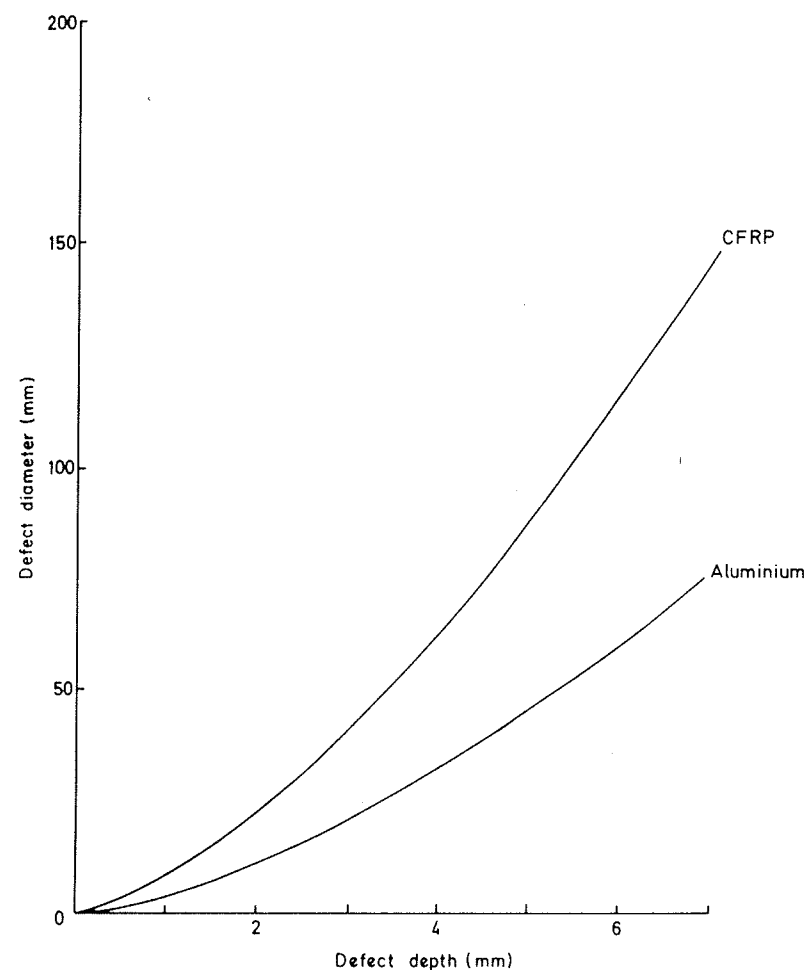


FIG. 37. Minimum detectable defect diameter versus defect depth in aluminium and CFRP for impedance method assuming 3 dB reliability in impedance measurement. Layer above defect modelled as plate with clamped edges. [After Cawley (1984).]

The technique is most sensitive if excitation is applied at the membrane resonant frequency. Since this frequency is dependent on defect size and depth, a broad band of frequencies must be covered. This was achieved in the Fokker Bond Tester Type 1 by using white noise excitation in a band from 0.5 to 10 kHz (Schliekelmann, 1972). Transmitting and receiving

piezoelectric probes were used and a meter displayed the ratio between the transmitted and received energy. It should be noted that this instrument is quite different from the widely used Fokker Bond Tester Type 2, which operates at much higher ultrasonic frequencies (200 kHz and upwards) and requires a couplant between the transducer and the structure.

It is also possible to use the technique with a single excitation frequency, though the sensitivity to flaws whose membrane resonant frequencies are far removed from the excitation frequency is considerably reduced. The Harmonic Bond Tester developed by Boeing and produced by the Shurtronics Corporation excites the laminate by induced eddy currents and measures the response with a microphone within the eddy current coil (Phelan, 1972). The interaction between the original and induced fields produces vibration excitation at double the frequency applied to the coil. The Harmonic Bond Tester uses a 15-kHz oscillator and so produces vibration excitation at 30 kHz. The eddy current excitation system cannot be used with nonconducting materials for which alternative excitation methods are employed. Botsco (1968) discussed a similar system but does allow the excitation frequency to be varied to suit the application. A single excitation frequency has also been used in the acoustic amplitude method developed by Lange (1976).

All the instruments discussed in this section are dependent on the membrane resonant frequency of the layer above the defect being close to the operating frequency range of the transducer. The membrane resonant frequency of a circular plate clamped around its edges is given by

$$f = (0.47h/a^2)\sqrt{E/\rho(1-\mu^2)}, \quad (21)$$

where h is the thickness of the layer above the defect, a is the defect radius and E , ρ and μ are the material modulus, density and Poisson's ratio, respectively. Thus a defect 1 mm deep and 5 mm in radius in aluminium has a membrane resonance at about 100 kHz. It is unlikely that any of the membrane resonance systems discussed above would detect this defect.

4. The acoustic spectral method

Lange (1978) has developed the Acoustic Spectral Flaw Detector, which was designed as an automated version of the coin-tap test discussed in section VI.B.1. The test area is tapped by an electromagnetically operated hammer and the resultant vibration is detected either by a microphone or by a piezoelectric transducer. The response signal is passed through a parallel set of filters to produce a response spectrum. This spectrum is then compared with that of an area which is known to be good.

The authors' work on the coin-tap test discussed in section VI.B.1 showed that the presence of a delamination or similar defect reduces the high-frequency energy present in the force pulse. This tends to reduce the amplitude of the response at high frequencies. However, Lange (1978) and Lange and Moskovenko (1978) report that the high-frequency response is frequently increased by the presence of a defect. This is because the membrane resonance of the layer above the defect falls within the frequency range investigated. Later work by Lange and Ustinov (1982) has shown that the presence of defects can either increase or decrease the response amplitude in different parts of the spectrum. The method therefore uses a combination of the change in input force due to damage and the membrane resonance effect discussed in section VI.B.3. There is a slight possibility that the effects might cancel out. These difficulties are avoided if the spectrum of the input force rather than the response is monitored as in the method proposed by Adams and Cawley (1983).

Response spectrum measurements have also been used to monitor the quality of civil engineering structures (Yamshchikov *et al.*, 1978).

5. Velocimetric methods

A number of techniques utilizing the effect of flaws on the wave speed and wave path length between transmitting and receiving piezoelectric transducers have been developed in the Soviet Union (Lange and Moskovenko, 1978; Vinogradov *et al.*, 1977). These use frequencies between 25 and 60 kHz which are higher than those used by most of the tests discussed earlier. The methods are more sensitive than the impedance technique discussed in section VI.B.2 but unless both sides of the component can be accessed, there is a dead zone adjoining the face opposite to the test surface which constitutes 20–40% of the thickness.

The Sondicator discussed by Chapman (1981) may also be termed a velocimetric technique.

C. General assessment of local measurement techniques

The most attractive local measurement techniques use a single excitation point and a noncontacting, scanning measurement system. Unfortunately, the equipment required tends to be very expensive. The thermographic system for local damping measurements will cost over £25,000, and if a holographic system is used for local amplitude measurements, the cost is likely to be even greater. However, in large-scale applications where the techniques have the required sensitivity, the cost will be justified.

The methods discussed in section VI.B require excitation at each test point and are therefore much slower. However, they have the advantage over higher-frequency ultrasonic inspection that a dry contact between the probe and the structure is satisfactory, and so no coupling fluid is required. They are therefore easier to apply, particularly *in situ*, for example, on an aircraft wing. The techniques are also more suited to the inspection of honeycomb constructions than the higher-frequency methods.

All the methods of section VI.B are used for finding defects such as disbands and delaminations, usually under fairly thin skins. The impedance method operates at a single excitation frequency so the computational requirements are small. This means that the probe can be moved over the surface of the structure giving a continuous reading. However, there are dangers in using only one frequency.

The automated coin-tap method requires a spectrum to be computed at each test point. This means that the inspection rate is approximately four positions per second. However, the reliability is improved by looking at more than one frequency and the tapping head only makes instantaneous contact with the structure which removes the alignment and static clamping force problems which can arise with the impedance technique.

The methods based on the membrane resonance of the layer above the defect are quick but problems arise with defects whose natural frequencies are above the frequency range of the instrument and the probability of missing defects is greatly increased if excitation is confined to a single frequency or a narrow band.

None of the methods discussed here will be universally applicable. However, the range of low-frequency techniques based on local measurements can make a valuable contribution in many industries. They are particularly useful with honeycomb constructions and composite materials where it is frequently necessary to detect delaminations and disbands in a plane parallel to the structure's surface. This is the type of defect to which these local techniques are most sensitive.

VII. CONCLUSIONS

The vibration techniques reviewed here make a very valuable contribution to NDT. The global methods involving measurements of natural frequencies and damping are extremely quick to carry out and give information about the integrity of the whole of the component from a single point test. They are not as sensitive to small localized defects as tests which involve point by point testing of the whole component, but their sensitivity is sufficient for many purposes and the speed and ease of testing which they offer means that their implementation is often worth investigating.

The local vibration techniques are particularly useful in circumstances where the use of the coupling fluids required for ultrasonic testing is undesirable. They are frequently used for the inspection of honeycomb constructions and composite materials.

The advent of microelectronics means that the cost and bulk of the equipment required to carry out vibration tests reliably and quickly is reducing rapidly. The time is therefore ripe for more attention to be paid to the opportunities which vibration techniques offer for improving inspection reliability and efficiency.

REFERENCES

- Adams, R. D. (1972a). *J. Sound Vibration* **23**(2), 199–216.
 Adams, R. D. (1972b). *J. Phys. D* **5**, 1877–1889.
 Adams, R. D. (1976). *In Proc. Int. Symp. on Nondestructive Control of Materials*, Bratislava, Czechoslovakia, 1976.
 Adams, R. D., and Bacon, D. G. C. (1973a). *J. Compos. Mater.* **7**, 53–67.
 Adams, R. D., and Bacon, D. G. C. (1973b). *J. Compos. Mater.* **7**, 402–428.
 Adams, R. D., and Cawley, P. (1983). UK patent application No. 8309030, March 1983.
 Adams, R. D., and Fox, M. A. O. (1973). *J. Iron Steel Inst.* **211**, 37–43.
 Adams, R. D., and Short, D. (1973). *J. Phys. D* **6**, 1032–1039.
 Adams, R. D., and Vaughan, N. D. (1981). *J. Non-Destr. Eval.* **2**, 65–74.
 Adams, R. D., Flitcroft, J. E., Hancox, N. L., and Reynolds, W. N. (1973). *J. Compos. Mater.* **7**, 68–75.
 Adams, R. D., Walton, D., Flitcroft, J. E., and Short, D. (1974a). *Compos. Reliab. ASTM Spec. Tech. Publ.* **580**, 149–175.
 Adams, R. D., Walton, D., and Short, D. (1974b). *In Proc. RILEM Symposium, New Developments in Nondestructive Testing of Non-Metallic Materials*, Constantza, Romania.
 Adams, R. D., Cawley, P., Pye, C. J., and Stone, B. J. (1978). *J. Mech. Eng. Sci* **20**, 93–100.
 Al-Agha, H. R., and Adams, R. D. (1982). *In Proc. 10th World Conference on NDT*, Paper 1A–26, Moscow.
 Bickford, R. H., Demchak, G. V., and Sciarra, J. J. (1973). "The Evaluation of the Acoustic Impact Technique for Detection of Incipient Cracks in Aircraft Components," AF-ML-TR-73-146.
 Birchon, D. (1964). *Eng. Mater. Des.* **7**, 692–696.
 Botsco, R. (1968). *Mater. Eval.* **26**, 21–26.
 Bray, A., and Gianasso, M. (1973). *Mater. Eval.* **31**, 145–151.
 Brown, R. J. (1973). *Non-Destr. Test.* **6**, 81–85.
 Brownjohn, J. M. W., Steel, G. H., Cawley, P., and Adams, R. D. (1980). *J. Sound Vibration* **73**, 461–468.
 Campbell, J. M., and McLachlan, E. H. (1979). *Br. J. Non-Destr. Test.* **21**, 71–75.

- Cawley, P. (1984). *NDT Int.* **17**, 59-65.
- Cawley, P. (1985). *I. Mech. E. Conf. Publ.* (In press.)
- Cawley, P., and Adams, R. D. (1978). *J. Compos. Mater.* **12**, 336-347.
- Cawley, P., and Adams, R. D. (1979a). *J. Strain Anal.* **14**, 49-57.
- Cawley, P., and Adams, R. D. (1979b). *J. Compos. Mater.* **13**, 161-175.
- Cawley, P., and Adams, R. D. (1979c). *Am. Soc. Mech. Eng. [Pap.]* 79-DET-46.
- Cawley, P., and Adams, R. D. (1979). *J. Sound Vibration* **64**, 123-132.
- Cawley, P., Woolfrey, A. M., and Adams, R. D. (1985). *Composites* **16**, 23-27.
- Chapman, G. B. (1981). *ASTM Spec. Tech. Publ.* 749, 32-60.
- Chondros, T. D., and Dimarogonas, A. D. (1980). *J. Sound Vibration* **69**, 531-538.
- Cochardt, A. W. (1953). *J. Appl. Mech.* **20**, 196-200.
- Coppolino, R. N., and Rubin, S. (1980). In Proc. 12th Annual Offshore Technology Conference, paper OTC 3865.
- Curtis, G. J., and Lloyd, P. A. (1980). *Chart. Mech. Eng.* (October), 55-60.
- Davis, A. G., and Dunn, C. S. (1974). *Proc. Inst. Civil Engineers* **57** (2) 571-593.
- Dousis, D. A., and Finch, R. D. (1980). *Am. Soc. Mech. Eng. [Pap.]* 80-WA/RT-2.
- Erf, R. K. (ed.) (1974). "Holographic Nondestructive Testing." Academic Press, New York.
- Ewins, D. J. (1976). *J. Soc. Env. Eng.* **15**, 23-30.
- Fagot, H., Albe, F., Smigielski, P., and Arnoud, J. L. (1980). "Holographic Nondestructive Testing of Materials using Pulsed Lasers", Institut Franco-Allemand de Recherches de Saint-Louis, Report No. CO 223/80.
- Finch, R. D., and Thomford, W. E. (1982). *ASME Pap.* 82-HH-62.
- Fox, M. A. O., and Adams, R. D. (1972). *J. Iron Steel Inst.* **210**, 527-530.
- Fox, M. A. O., and Adams, R. D. (1973). *J. Mech. Eng. Sci.* **15**, 81-94.
- Fresch, D. C., Yaeger, L. L., and Hochrein, A. A. (1978). DAI-DF-7763-001-TR.
- Goodwin, R. J. (1968). *Met. Sci. J.* **2**, 121-128.
- Guild, F. J., and Adams, R. D. (1981). *J. Phys. D* **14**, 1561-1573.
- Hagemaiier, D., and Fassbender, R. (1978). *SAMPE Q.* (July), 36-58.
- Henneke, E. G., and Jones, T. S. (1978). *ASTM Cttee. D-30 Conf. On NDE and Flaw Criticality for Composite Materials, Philadelphia.*
- Hochrein, A. A., and Yeager, L. L. (1978). "Computer Assisted Digital Processing System for Non-destructive Evaluation Technique Utilizing the Phenomenon of Internal Friction", Fracture Mechanics Symposium on Naval Structure Mechanics, George Washington University, September 1978. University Press of Virginia.
- Hoffman, B. (1972). *Mater. Res. Stand.* **12**, 17-20.
- Hoffman, B., and Addison, H. J. (1974). In Proc. Conf. on Automated Inspection and Production Control, Chicago.
- Kenley, R. M., and Dodds, C. J. (1980). In Proc. 12th Annual Offshore Technology Conference, paper OTC 3866.
- Konovalova, T. A., Aronson, E. V., and Burinskaya, V. V. (1973). *Refractories* **14**, 283-285.
- Lange, Yu V. (1976). *Soviet J. Nondestr. Test. (Engl. Transl.)* **12**, 5-11.
- Lange, Yu V. (1978). *Soviet J. Nondestr. Test. (Engl. Transl.)* **14**, 634-643.

- Lange, Yu V., and Moskovenko, I. B. (1978). *Soviet J. Nondestr. Test. (Engl. Transl.)* **14**, 788-797.
- Lange, Yu V., and Teumin, I. I. (1971). *Soviet J. Nondestr. Test. (Engl. Transl.)* **7**, 157-165.
- Lange, Yu V., and Ustinov, E. G. (1982). *Soviet J. Nondestr. Test. (Engl. Transl.)* **18**, 11-14.
- Lazan, B. J. (1968). "Damping of Materials and Members in Structural Mechanics." Pergamon, London.
- Lilley, D. M., Adams, R. D., and Larnach, W. J. (1982). Paper 3-4, 10th Word Conf. on NDT, Moscow.
- Lloyd, P. A., Joinson, A. B., and Curtis, G. J. (1975). In Proc. Ultrasonics International 68-72.
- Lloyd, P. A., Joinson, A. B., and Curtis, G. J. (1976). In Proc. 8th World Conf. on NDT, Cannes, France, Paper 3K8.
- Loland, O., and Dodds, C. J. (1976). Offshore Technology Conference, paper OTC 2551.
- Loland, O., and Mackenzie, A. C. (1974). *Mech. Res. Commun.* **1**, 353-354.
- Loland, O., Begg, R. D., and Mackenzie, A. C. (1975a). "The dynamic response of a fixed steel offshore oil platform." BSSM/RINA Conf., Edinburgh.
- Loland, O., Mackenzie, A. C., and Begg, R. D. (1975b). "Integrity monitoring of fixed steel offshore oil platforms." BSSM/RINA Conf., Edinburgh.
- Magistrali, G. (1975). *Non-Destr. Test.* **8**, 32-37.
- Mayes, I. W., and Davies, W. G. R. (1976). I. Mech. E. Conf. on Vibrations in Rotating Machinery, paper C168/76, Cambridge.
- Nagy, K., Dousis, D. A., and Finch, R. D. (1978). "Detection of flaws in railroad wheels using acoustic signatures." *J. Eng. Ind.* **100**, 459-467.
- Nevadunsky, J. J., Lucas, J. J., and Salkind, M. J. (1975). *J. Compos. Mater.* **9**, 394-408.
- Ni, R. G., and Adams, R. D. (1984). *J. Compos. Mater.* **18**, 104-121.
- Olver, L., Brasfield, R. G., Yeager, L. L., and Thiruvengadam, A. P. (1980). "Application of internal friction non-destructive evaluation technique for wire ropes used in mining operations." DAI Technical Report, LLY-7813-001-TR.
- Peters, J., Snoeys, R., and Decneut, A. (1969). In "Advances in Machine Tool Design and Research." (S. A. Tobias and F. Koenigsberger, eds.) Proc. 9th Int. MTDR Conf., Part 2, 1968. Pergamon, Oxford.
- Peterson, E. L., and Klosterman, A. L. (1978). *J. Soc. En. Eng.* **17**.
- Phelan, C. S. (1972). Applied Polymer Symposium No. 19, pp. 423-439, Wiley, New York.
- Pisarenko, G. S. (1962). "Dissipation of energy during mechanical vibration." Trans. Ukrainian Academy of Sciences publication.
- Pye, C. J., and Adams, R. D. (1981a). *NDT Int.* **14**, 111-118.
- Pye, C. J., and Adams, R. D. (1981b). *J. Phys. D* **14**, 927-941.
- Pye, C. J., and Adams, R. D. (1982). *Eng. Fract. Mech.* **16**, 433-445.
- Randall, R. B. (1977). "Application of Bruel and Kjaer Equipment to Frequency Analysis." Bruel and Kjaer, Copenhagen.

- Reifsnider K. L., and Stinchcomb, W. W. (1976). *In Proc. Infrared Information Exchange*.
- Reifsnider, K. L., and Williams, R. S. (1974). *Exp. Mech.* **14**, 479-485.
- Savage, R. J., and Hewlett, P. C. (1978). *NDT Int.* **11**, 61-67.
- Schliekelmann, R. J. (1972). *Non-Destr. Test.* **5**, 144-153.
- Schroerer, R. (1970). *Non-Destr. Test.* **3**, 194-196.
- Schroerer, R., Rowand, R., and Kamm, H. (1970). *Mater. Eval.* **28**, 237-243.
- Shaw, D. A. (1974). *IEEE Trans. Instrum. Meas.* **IM-23**, 240-244.
- Shen, C. H. (1982). "Grinding wheel screening by the elastic modulus method." *Inspection and Quality Control in Manufacturing Systems*, PED, Vol. 6. Presented at Winter Meeting, ASME, Phoenix.
- Spain, R. F., Schubring, N. W., and Diamond, M. J. (1964). *Mater. Eval.* **22**, 113-117.
- Sumner, G., and Entwistle, K. M. (1959). *J. Iron Steel Inst.* **192**, 238-245.
- Timoshenko, S. P. (1937). "Vibration Problems in Engineering." Van Nostrand-Reinhold, Princeton, New Jersey.
- Uygur, E. M. (1980). *In "Research Techniques in NDT"* (R. S. Sharpe, ed.), Vol. 4, Academic Press, London.
- Vinogradov, N. V., Tsorin, E. I., Filimonov, S. A., Lange, Yu.V., and Murashov, V. V. (1977). *Soviet J. Non-Destr. Test. (Engl. Transl.)* **13**, 93-96.
- Yamshchikov, V. S., Sisorov, E. E., Baukov, Yu.N., and Potapov, V. S. (1978). *Soviet J. Non-Destr. Test. (Engl. Transl.)* **14**, 696-702.
- Yeager, L. L., *et al.* (1981). "Application of the internal friction damping non-destructive evaluation technique for identification of degradation and failure of shipboard cargo piping." Daedalean Associates, Inc., Woodbine, Maryland, P.B.82 108879.

CHAPTER 8

Automated Visual Inspection

C. C. BOWMAN

Auckland Industrial Development Division, Department of Scientific and Industrial Research, Auckland, New Zealand

and

B. G. BATCHELOR

University of Wales Institute of Science and Technology, Cardiff, UK

I. Introduction	361
II. Techniques	365
A. Mechanical handling	366
B. Illumination	367
C. Optics	375
D. Image acquisition	379
E. Image analysis	382
III. Applications	415
A. Commercial AVI systems	415
B. Application areas	416
C. The UWIST laboratory	419
IV. AVI in the future	419
References	421
Bibliography	423

I. INTRODUCTION

The importance of inspection in the quality assurance of manufactured products is well understood. Rapid advances in the automation of production methods have increased inspection requirements for two main reasons. Firstly, higher production speeds require higher inspection speeds. Secondly, the implicit inspection involved in manual production and as-